



State-of-art review on smart perovskites materials: properties and applications

Priyanka Thakur¹ · Navdeep Sharma² · Dinesh Pathak³ · Pankaj Sharma⁴ · Kamal Kishore⁵ · Shashi Dhar⁶ · Madan Lal⁷

Received: 14 November 2023 / Accepted: 5 February 2024 / Published online: 26 February 2024
© Qatar University and Springer Nature Switzerland AG 2024

Abstract

Materials science has played a very crucial role in developing new technologies so far that could probably address the challenges of economic and ecological sustainability soon. In the field of advanced materials, perovskite oxides stand out to provide a clean environment, ensure enough clean energy, and sanitized water, and provide resources for industrial and growing populations. Perovskite oxides are green and eco-friendly smart materials whose properties might be significantly altered under controlled conditions. In this regard, lead-free perovskite ceramics and their composites such as BaTiO_3 , $\text{K}_{0.5}\text{Na}_{0.5}\text{NbO}_3$, $\text{Bi}_{0.5}\text{Na}_{0.5}\text{TiO}_3$, LaMnO_3 , BaMnO_3 , LaFeO_3 , $\text{K}_{0.5}\text{Na}_{0.5}\text{NbO}_3\text{-BiFeO}_3$, $\text{BaTiO}_3\text{-K}_{0.5}\text{Na}_{0.5}\text{NbO}_3$, $\text{BaTiO}_3\text{-Bi}_{0.5}\text{Na}_{0.5}\text{TiO}_3$, and many more are gaining attention due to their simple stoichiometry, cost-effectiveness, easy synthesis, eco-friendly behavior, and world-wide applications. In this review, a brief overview is given of the crystal structure and piezoelectric, ferroelectric, magnetic, and multiferroic properties of perovskite oxides. An attempt has been made to cover the progress of selective perovskite oxide and its composites. The recent advances of these perovskite oxides and applications in energy storage, energy scavenging applications via multi-layer ceramic capacitors, supercapacitors, solid-oxide fuel cells, piezoelectric actuators, transducers, sensors, and spintronics are also highlighted. Moreover, recent industrial developments based on these selective perovskite oxides are discussed as well. At the end of this review, future perspectives on current developments of perovskite oxides are also evaluated.

Keywords SDGs · Antiferromagnetic · Relaxor · Superexchange multiferroic · Supercapacitors

1 Introduction

In a world with energy crises, pollution, water contamination, and climate change, choosing an alternative has become essential for all living beings. Various natural and human conducts are responsible for accelerating these issues. However, for the betterment of the world, different initiatives have been taken so far. Laws enforced by governments and different social activities have successfully brought awareness among the people. These are the direct initiatives that highly impact the world population, aware and educate them about their participation in resolving these issues, and are responsible for choosing green alternatives for the environment and society [1]. Sustainable Development Goals (SDGs) are one of the direct initiatives which encapsulate almost all global issues from ending poverty to protecting the planet. The recognized 17 SDGs integrate that action in one area will affect outcomes in others, and the development will balance social, economic, and environmental

✉ Madan Lal
madan.physics26@gmail.com

- ¹ Department of Physics, Akal College of Basic Sciences, Eternal University, Sirmour, HP 173101, India
- ² Department of Physics, School of Basic Sciences, Abhilashi University, Mandi, HP 175045, India
- ³ Department of Physics, The University of the West Indies, Saint Augustine 32080, Trinidad and Tobago
- ⁴ Applied Science Department, National Institute of Technical Teachers Training and Research, Chandigarh 160019, India
- ⁵ Department of Chemistry & Biochemistry, Akal College of Basic Sciences, Eternal University, Sirmour, HP 173101, India
- ⁶ Himachal Pradesh Council for Science, Technology & Environment (HIMCOSTE), Shimla, HP 171009, India
- ⁷ Department of Allied Sciences (Physics), Graphic Era (Deemed to be University), Clement Town, Dehradun UK-248002, India

sustainability. Adopted in 2015 by the United Nations, these SDGs are supposed to be attained by 2030, to ensure peace and prosperity in the world [2].

Science is a dynamic connection between knowledge and action which can indirectly affect the process of achieving SDGs. Due to its ability to lay foundations for new approaches and solutions, science is critical to tackling complex challenges for humanity such as climate change, pollution, biodiversity loss, and poverty reduction. Science, technology, and innovation (STI) are considered central tools for SDG implementation as they can be used to achieve all the SDGs that fall under the social and environmental pillars of sustainable development [3]. Material science plays a very crucial role in developing new technologies that could probably address challenges of economic and ecological sustainability. Clean energy production, carbon sequestration, delivery of sanitized water, and antimicrobial action are the key areas where advanced materials have the potential to make a solid impact in meeting SDGs by 2030 [4].

Transition metal dichalcogenides, and specifically, molybdenum disulfide (MoS_2) in terms of structure and their application as an effective energy storage material. They consist of weakly joined sandwich-like layers (X-M-X). The neighboring layers are connected via van der Waals forces. In each layer, M is bonded to X atoms by covalent bonds. Exfoliation of the bulk substances into a few layers mostly conserves their characteristics and leads to additional features due to restriction impacts. These materials have sparked numerous interests due to their unique physical characteristics and special applications. Thus, as one of this family, MoS_2 has recently been broadly studied in many research fields, such as lubrication, supercapacitors, lithium-ion batteries, and drug delivery because of its extraordinary activity and its perfect two-dimensional structure. MoS_2 has also exhibited excellent performance in environmental remediation applications such as electro- or photocatalysis, adsorption of heavy metals, ammonium nitrogen removal, and membrane-based separation [5].

Similarly, in the field of advanced materials, perovskite oxides stand out to provide a clean environment, sanitized water, and ensure enough clean energy and resources for industrial and population growth. These materials have been widely investigated over the last 70 years due to their multiple properties contained in a single material. However, technology based on perovskite materials has still not reached commercialization. Perovskites have a wide range of properties, such as electronic and ionic conductivity, piezoelectricity, magnetic properties, superconductivity, and catalytic activity [6]. Owing to these properties, they tend to improve conventional well-known technologies and facilitate novel technologies. The application of perovskites in biomaterials and smart drug delivery [7], solid oxide fuel end electrolysis cells (SOFCs) [8], Ca batteries [9], magnetic data storage

and spintronics [10], magnetic refrigerators [11], catalysis [12], can be used to achieve sustainable growth and development by 2030.

The structural family of perovskite material is considered the most promising family and is categorized as a smart material due to its superior properties and wide range of applications. The eco-friendly nature of perovskite materials makes them promising candidates for different biochemical and industrial applications. In nature, perovskite is primarily found as oxides, mostly silicates, but they also exist as fluorides, sulfides, and intermetallic compounds. Naturally occurring perovskites are limited but synthetic perovskite materials can accommodate almost all the elements of the periodic table which makes them the most versatile material. Over the past few decades, perovskite materials have traditionally been used as functional materials in energy-related fields. These materials exhibit an array of electrical, chemical, and magnetic properties which make them fascinating materials for studies and apply to a large scale. The first discovered perovskite was CaTiO_3 , also termed mineral perovskite, which was found by Geologist Gustav Rose in 1839 [13]. The name perovskite came after the first discoverer Count Lev Alexevich von Perovski. All the materials that show the structure like CaTiO_3 are termed Perovskites. ABX_3 is a general chemical formula for all perovskite materials with an ideal cubic structure at room temperature. Cubic structure is not very stable even mineral perovskite itself has some distortions in the structure. These structural distortions have a positive impact on the ferroelectric, and piezoelectric properties which are responsible for the energy storage and energy harvesting applications of these materials.

There are several excellent reviews available in the literature on perovskite materials that give an overview of the selected properties and their applications. The present review will provide a detailed state of art review of perovskite materials with different properties and applications in various technological fields. The present study will focus on the materials that exhibit various properties that can be utilized in energy storage and energy scavenging applications. Selective materials (BaTiO_3 , KNN, BNT, BiFeO_3 , LaMnO_3 , BaMnO_3 , LaFeO_3 , and their based perovskite material along with composites) will be reviewed in the following sections, to provide a detailed analysis of these materials and their related applications that may lead to attaining SDGs will be discussed.

1.1 Crystal structure of perovskite

ABX_3 is the general formula for all the perovskite compounds, where A and B cations are of different ionic radii (A cation with bigger ionic radii) and X is an anion mostly oxide, sulfide, halide, or nitride. A, B, and X can represent a combination of different organic and inorganic ions thus

perovskite compounds are classified as inorganic oxide perovskites, alkaline metal halide perovskites, and organic metal halide perovskites [14].

Inorganic oxide perovskite also known as ceramic perovskite has a generic form ABO_3 in which A ion is an alkali earth metal (Ca, Ba, Sr) or lanthanides (La, Ce, Nd) with a larger radius, B is a transition metal ion (Mn, Ti, Fe) with a smaller radius and O is an oxygen ion with 1:1:3 composition. In the cubic unit cell of ABO_3 perovskite, A ions are located at the cube corner position, B ions occupy the body center, and the oxygen ions are at the face-centered position of the unit cell as shown in Fig. 1. A stable perovskite structure is formed by the 12-fold coordination of A cation and the sixfold coordination of B ions which are surrounded by an octahedron of oxygen anions [15, 16].

1.1.1 Distortions in the ideal perovskite structure

The ideal cubic perovskite structure is not very common even mineral perovskite itself is slightly distorted. These distortions occur by tilting of $[BO]_6$ octahedral due to different effects such as a change in temperature, the presence of spontaneous polarization, stress, or strain in the material, etc. In a tilted octahedral system, some of the A–O distances become smaller while some become longer which reduces the effective coordination of the A-cations environment. The structural distortion leads to a change in crystal structure from ideal cubic to orthorhombic, rhombohedral, hexagonal, or tetragonal form as shown in Fig. 2. For the formation of a stable perovskite structure, two requirements should be fulfilled [17]:

1. Electro-neutrality: An appropriate charge distribution must be attained to form a stable perovskite structure.

Electro-neutrality implies that the total charge on cations (A and B) must be equal to the total charge on anions.

2. Size effect: V. M. Goldschmidt [18] presented that empirical ionic radii at room temperature are defined by tolerance factor (t) and given by:

$$t = r_A + r_O / \sqrt{2r_B + r_O}$$

where r_A , r_B , and r_O are the radius of ions A, B, and O ions respectively. Tolerance factor (t) increases with an increase in ionic radii of A cation (r_A) and decreases with a decrease in ionic radii of B cation (r_B); hence, it is also used to describe the combination of cations for perovskite structure [19]. The t -factor is used to measure the degree of distortion of perovskite structure from its ideal cubic form. As the value of t deviated from unity the ideal cubic structure is changed to rhombohedral, orthorhombic, or tetragonal structures (as shown in Fig. 2). For $1 < t < 1.13$ the perovskite structure is hexagonal, for $0.9 < t < 1.0$, it is cubic and for $0.75 < t < 0.9$, the structure is orthorhombic. For $t < 0.75$, it shows a hexagonal ilmenite structure [20]. Ideal perovskite structure is obtained if the value $r_A > 0.09$ nm, $r_B > 0.051$ nm, and the tolerance factor lies between $0.8 < t < 1.0$.

Perovskite materials form the building blocks for other important crystal structures such as Ruddlesden-Popper phases, Aurivillius compounds, and oxygen-deficient brownmillerite compounds [21]. The distortions in these crystal structures are due to the appearance of spontaneous polarization.

Fig. 1 Ideal perovskite crystal structure

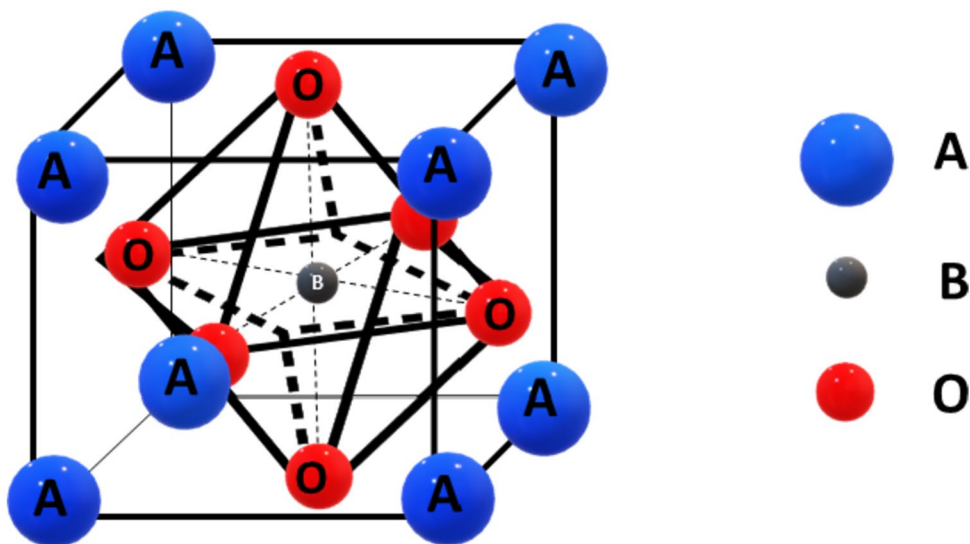
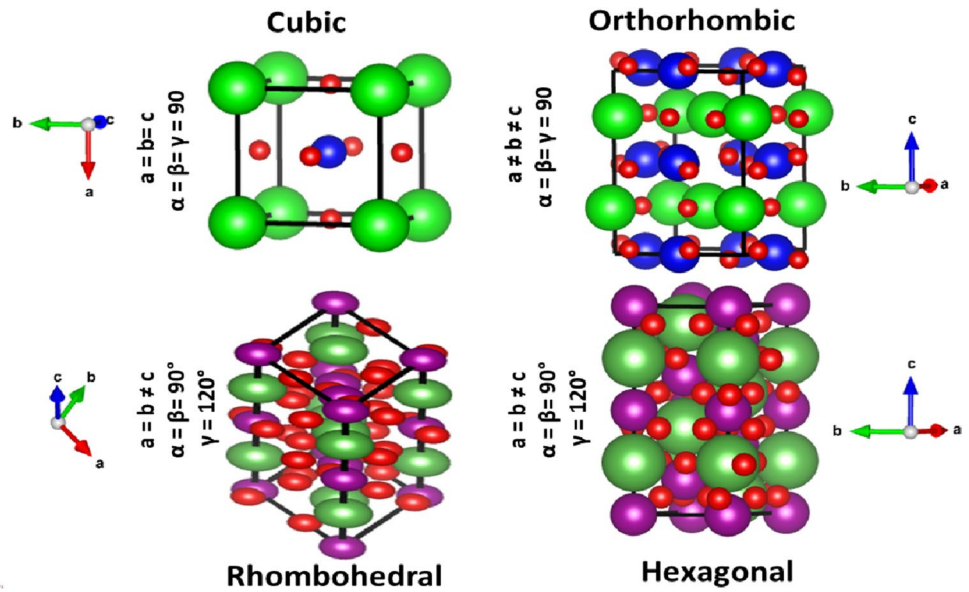


Fig. 2 Change in structure from ideal cubic phase



1.1.2 Effect of temperature on the crystal structure

A perovskite crystal structure is also sensitive to temperature. It shows different phases under temperature variations. Generally, at higher temperatures, the tilting of BO_6 octahedra is observed which is found to be the reason for the change in crystal structure. For example, BaTiO_3 assumes five different crystal structures namely hexagonal, cubic, tetragonal, orthorhombic, and rhombohedral at different temperatures. The hexagonal structure is stable above 1460°C , while the tetragonal phase occurs on cooling BaTiO_3 below 1460°C . This tetragonal phase is stable until 0°C , where it transforms into an orthorhombic phase. The structural transformation of BaTiO_3 is shown in Fig. 3 [22].

1.2 Other factors that affect the perovskite structure

Along with size effect, electro-neutrality, and temperature, other factors are responsible for the distorted structure of perovskites.

1.2.1 Composition change from ideal ABO_3

If a cation with multiple oxidation states like Fe in SrFeO_3 with +2 and +3 oxidation states is present in the structure then due to heating a sample in an oxidizing and reducing environment the valency of the cation is changed which results in structure deviation from cubic to another phase. This leads to a change in the oxygen content in between 2.5 and 3. For example in SrFeO_x ($2.5 \leq x \leq 3$), some Fe ions

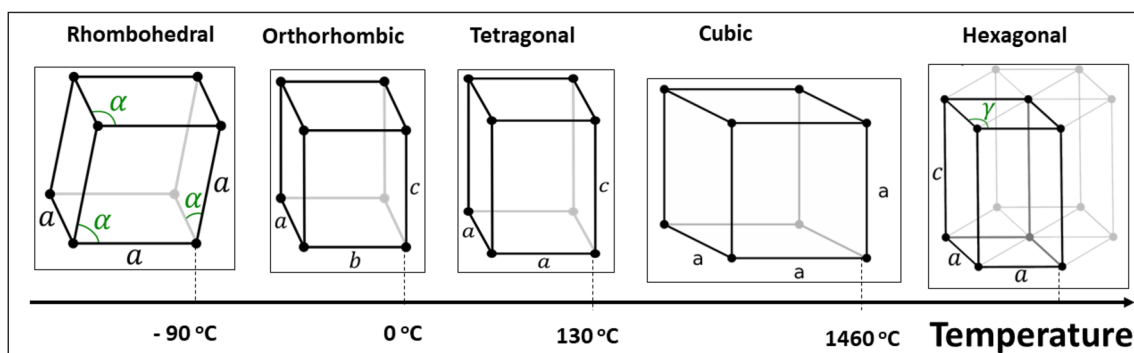


Fig. 3 Phase diagram of BaTiO_3

can be assigned to the +3 oxidation state while others to +4 which results in structure deformation. These compounds are the example of defective perovskites.

1.2.2 Jahn–Teller effect

The distortion in perovskite structure can be assigned to Jahn-Teller active ions at the B site such as Mn^{3+} . In this case, the d orbital electrons are divided up into e_g and t_g orbitals, and an odd number of electrons in e_g orbitals are the reason for the elongation of $[Bo_6]$ octahedra. For example, $LaMnO_3$ has Mn^{3+} at the B site and has one unpaired electron in e_g orbit which results in a deviation from cubic structure to hexagonal.

These distortions result in reduced symmetry of crystal structures of perovskite materials and influence various physical, chemical, electrical, and magnetic properties of these materials. Because of various properties, perovskite materials have replaced different materials in various technological applications. For instance, after the discovery of lead zirconate titanate in 1954, it has dominated almost all the electronic market due to its high dielectric constant, high piezoelectric coefficient, and high Curie temperature. For energy harvesting applications, PZT-5 h and PZT-5A materials have been widely used to fabricate energy harvesters for generating power of the order of milliwatts. However, because of lead oxide toxicity, the European community explicitly limits the use of Pb in electronic equipment.

During the processing at a higher temperature, lead oxide vaporizes and remains in the environment for a long time, which accumulates in the organisms and causes health hazards, thus recycling and disposal of PZT-based devices especially those used in cars, sound generators, and various kind of smart devices is a rising concern. These restrictions on the use of certain hazardous substances make the researchers focus on lead-free piezoelectric materials such as BNT, KNN, and BTO. To prohibit the use of Pb in electronic devices, related laws and regulations such as “The Restriction on the use of certain Hazardous substances in Electrical and Electronic Equipment (RoHS) and Waste Electrical and Electronic Equipment (WEEE) have been legislated and make it necessary to develop Pb-free materials for sustainable development.

Magnetic properties of perovskite materials such as $LaMnO_3$, $BaMnO_3$, and $LaFeO_3$ are exploited for spintronics applications in mass storage devices, magnetic readers, memory devices, and cancer detection devices. Antiferromagnetic which were initially considered as not-so-useful materials have recently found potential advantages in spintronic devices over conventional ferromagnets. Perovskite oxides are exploited as an electrode, electrolyte, and dielectric material, in energy conversion and energy storage applications via solar cells, solid oxide fuel cells (SOFC),

batteries, and supercapacitors. Various properties of perovskite materials are discussed in the following sections.

1.3 Effect of crystal structure on various properties

As discussed, the perovskite crystal structure directly or indirectly depends upon the various factors hence perovskites can crystallize in all possible symmetries, from high symmetry cubic to very low symmetry triclinic. Various properties associated with these materials are highly influenced by crystal symmetry such as piezoelectric, ferroelectric, and magnetic. For example, dielectric properties like piezo and ferroelectricity are more prominent in the materials with the lowest symmetry. Therefore, perovskite crystal structure with low symmetry such as orthorhombic, tetragonal, and triclinic shows higher piezoelectric and ferroelectric properties than cubic. Similarly, the fundamental requirement for magnetic property is the highest symmetry hence cubic perovskite materials show high magnetic moments compared to others. All these properties along with various examples are discussed in the following section.

2 Properties of perovskite oxides

Perovskite materials have drawn intensive attention due to their cost-effectiveness, easy synthesis, and wide variety of properties in a single material. Along with dielectric properties like piezo, ferro, and pyroelectricity, these materials show excellent mechanical and chemical activity. Photocatalysis using perovskite semiconductors, electrode materials in Supercapacitors, high permittivity perovskite materials, and multiferroic perovskite materials have been widely studied. These properties are highly dependent on the non-stoichiometry of anions or cations, the valance state of the electronic structure, distortion in the perovskite structure, and the mixed valance state.

2.1 Piezoelectricity

Piezoelectricity was found in perovskite materials in 2000, since then the studies into lead-free piezoelectric materials have grown exponentially. Piezoelectric materials generate electric signals from the application of mechanical stress termed as direct piezoelectric effect (as shown in Fig. 4). The piezoelectric material, when subjected to mechanical strain, gets polarized and produces electric signals, and the degree of polarization of the material is proportional to the applied strain.

$$\Delta P \propto T$$

or

$$\Delta P = dT$$

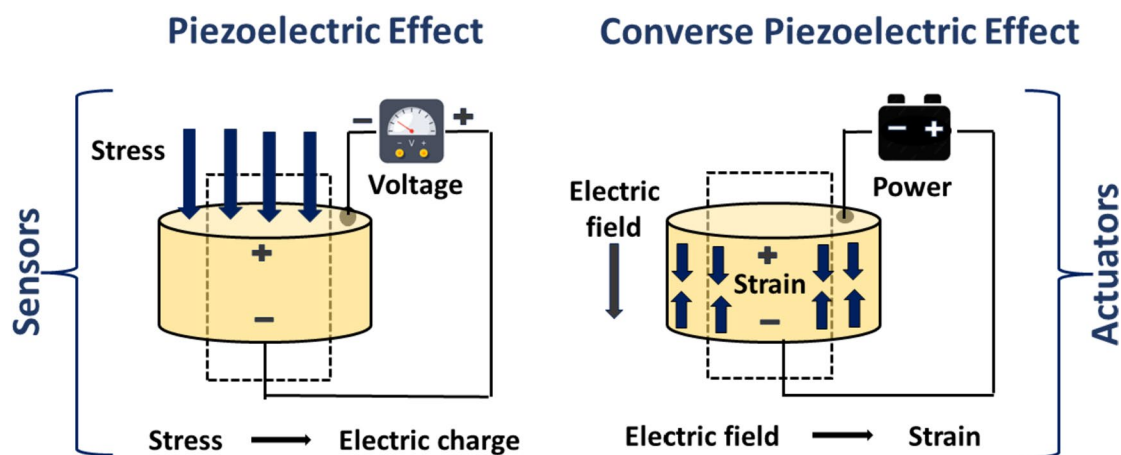


Fig. 4 Schematic representation of piezoelectric and converse piezoelectric effect

where ΔP (Cm^{-2}) is the change in polarization, T (Pa) is Mechanical Pressure, and d (CN^{-1}) is the proportionality constant known as the piezoelectric charge coefficient.

The converse of the piezoelectric effect is also true and is known as the converse or indirect piezoelectric effect. An external electric field results in mechanical deformation in the crystal lattice (as shown in Fig. 4). Generally, mechanical deformation is linearly proportional to the applied electric field.

$S \propto E$

or

$$S = dE$$

where S is mechanical strain, E (Vm^{-1}) is the electric field, and d (mV^{-1}) is the piezoelectric coefficient same as for the direct effect.

Quartz, cane sugar, collagen, topaz, Rochelle salt, tendon, etc. are naturally occurring piezoelectric materials. BaTiO_3 and BNT, KNN-based ceramics with perovskite structure, exhibit excellent piezoelectric properties. These materials are the most studied because of their large piezoelectric coefficient values, electromechanical coupling factor near 1, and high efficiency. These properties show many valuable scientific applications such as sensors, microphones, high voltage, and power sources, actuators, piezoelectric motors, nano-positioning in AFM, transducers, and energy harvesting [23].

Piezoelectricity is associated with the crystallographic symmetry of different materials hence it is related to the internal structure of a material. As is well known, a material has a definite chemical composition and is made up of positive and negative ions. These ions occupy specific positions and repeat themselves in 3-dimensional space forming a crystal lattice. The smallest unit of the lattice that repeats itself in 3D space is called a unit cell. These are the building

blocks of the crystal lattice, and some symmetry operations are associated with the unit cell of a crystal structure about a point in space. According to Neumann's principle, the symmetry possessed by the internal structure of a material is reflected in the symmetry of the external properties of that material. Thus, specific symmetries possessed by the internal structure of a material determine the piezoelectric properties of the materials.

2.2 Ferroelectricity

The materials that show spontaneous polarization, which can be reversed under the effect of an external electric field, are known as ferroelectric materials. These are the insulating materials with high dielectric constant and are used in several applications like ultrasonic imaging devices, fire sensors, infrared cameras, RAM and memory devices, tuneable capacitors, vibrational sensors, etc. [24]. The dielectric constant of ferroelectric materials is twice as large as those of ordinary dielectric materials which makes these materials compelling for investigation. The large dielectric constant is due to the collective polar displacement of metal ions concerning oxygen ions.

The $[\text{BO}_6]$ octahedra plays a very vital role in ferroelectric transitions. When an external field is applied to the material, the B-site ions move to a new position along the direction of the applied field. The individual ionic movements approximate the alignment with the applied field because the crystallites or unit cells are randomly orientated, and the ions are constrained to move only along certain crystallographic directions. However, when the ionic movement occurs, it leads to dimensional changes in the unit cell along the direction of the applied field. The adjacent unit cells switch along the direction of the applied field as well are referred to as domain reorientation or switching.

Domains are the homogeneous areas of the materials with the same polarization orientations separated by the domain walls from the areas of unlike polarizations [25] as shown in Fig. 5. Domains are the names given according to the angle between the polarizations between adjacent regions. Hence, two adjacent regions in which the polarizations are orientated at 180° to each other are, naturally, called 180° domains. Domains are also classified as strain-producing domains and nonstrain-producing domains. For instance, in rhombohedral material 7° and 109° domains are strain-producing while 180° domains are nonstrain-producing.

2.2.1 Basic ferroelectric characteristics

a) Ferroelectric hysteresis

Switchable polarization that is the variation of polarization with electric field is not linear but forms a closed loop called the hysteresis loop. Figure 6 shows a schematic plot of polarization versus electric field as would be observed in typical ferroelectric materials. As the field is increased from zero, the polarizations in different dipolar regions are aligned with the field, and overall polarization in the crystal increases. Eventually, it reaches a saturation point at which all the dipolar regions are aligned. The only further increase in polarization after the saturation point is due to the relative permittivity of the material. Extrapolation of this line back to the y-axis gives the saturation value of the spontaneous polarization (P_s). When the external field is decreased even removal of the field that is at $E=0$, the

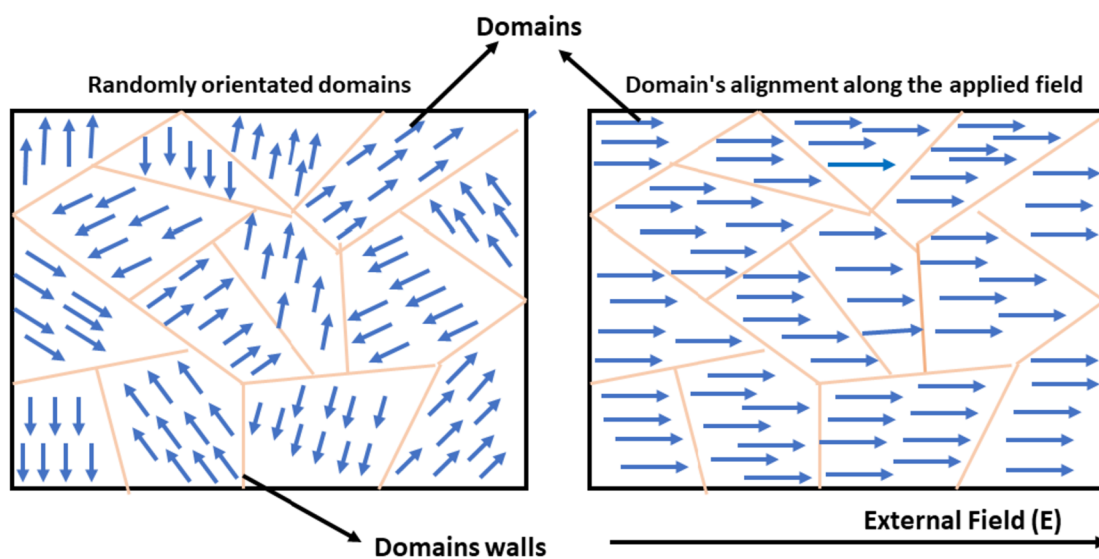
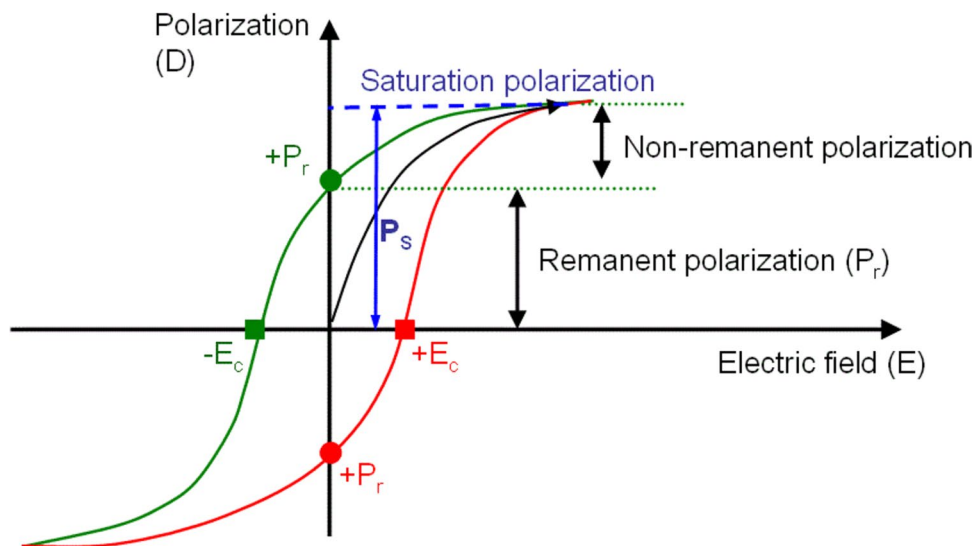


Fig. 5 Domain configuration for polycrystalline ferroelectric materials

Fig. 6 Ferroelectric hysteresis loop [26]



polarization remains in the material known as a remanent polarization (P_r), which is usually slightly less than P_s .

When the direction of the field is reversed, a negative field is applied the dipoles start to reorient which will cause the polarization to reduce, until it reaches zero at the coercive field ($-E_c$) where all the dipole regions are again randomly orientated. A further negative increase in the field will eventually cause a reverse saturation polarization ($-P_s$) to develop. When the field returns to zero the crystal is left with a negative remanent polarization ($-P_r$). Increasing the field once more increases the polarization from $-P_r$ to zero at E_c , and then to $+P_s$, completing the ferroelectric hysteresis loop. The ability to switch the polarization between two states gives rise to the first application of ferroelectrics as a non-volatile memory storage medium. The fact that polarization can possess different directions within different regions of the same crystal confirms the existence of ferroelectric domains [27].

b) Phase transitions

Solid-state phase transition is a correct interpretation and vital in revealing the physical nature of ferroelectricity. For almost every ferroelectric material, the polar state of a crystal in which the center of positive charge does not coincide with the center of negative charge only exists over a limited range of temperatures. As the temperature is raised above a certain critical point, the polar ferroelectric phase changes to a non-polar ferroelectric phase termed as paraelectric phase. The temperature at which the transition from ferroelectric to paraelectric phase occurs is known as Curie temperature (T_c) or critical temperature [28]. Mathematically, Curie temperature is a singular point concerning the dielectric permittivity.

Phase transition is characteristic of ferroelectric materials; however, some ferroelectric materials melt or decompose before the T_c is reached. The dielectric permittivity values are very high around T_c and decrease above this temperature which exploited the use of ferroelectric materials as a dielectric in high-value capacitors. The ferroelectric material in which dielectric permittivity values increase with the increasing temperature, reaching a peak at T_c and decreasing above this temperature, is known as proper ferroelectric materials, while some ferroelectric materials for which there is no peak of permittivity around T_c , but just an anomaly, termed as improper or extrinsic ferroelectrics.

The paraelectric phase is the phase with higher crystal symmetry. Once this phase is reached all the electric dipoles are in their non-polar form and the crystal structure becomes centrosymmetric. A crystal structure with the center of symmetry implies that for every atom in the structure, there exists a point in the unit cell through which inversion will bring one to the same type of atom. Normally, ferroelectrics are classified into two categories according to their phase

transitions: one with a first-order phase transition and the other with a second-order phase transition [29]. The difference between these two categories arises from the magnitude of dielectric permittivity during the transition. The first-order phase transition results in a finite value of the permittivity during the transition, while the second-order is accompanied by an infinite value of the permittivity. The fundamental physics behind normal ferroelectric lies in the presence of long-range order parameters or electric dipoles in ferroelectric domains [30].

2.2.2 Relaxor ferroelectrics

Among the ferroelectric materials, there exists a relaxor ferroelectric materials, the name assigned to the materials that fulfill the following three features [31]:

- (i) The temperature-dependent dielectric permittivity evinces a diffuse phase transition that is broad and smeared maxima around T_c (as shown in Fig. 7).
- (ii) The temperature corresponds to maximum dielectric permittivity is frequency dependent that is the presence of dielectric relaxations.
- (iii) There are no macroscopic symmetry breaking or structural changes near maximum dielectric temperature.

The relaxor ferroelectrics show abnormal behavior compared to normal ferroelectric in terms of dielectric, ferroelectric, and piezoelectric properties and have drawn much attention due to their applicability in portable electronics, medical devices, electric vehicles, pulse power devices, advanced strong materials, and so on [32]. The origin of relaxor ferroelectrics has been correlated with the presence of compositional fluctuations which induce the polar nanoregions (PNRs); however, the origin and underlying mechanism for the features in the relaxor materials is still a matter of debate.

The diffuse phase transition model the super-paraelectric model, the dipolar glass model, the random-field model, the random-site model, the bi-relaxation model, and the spherical-random-bond and random-field model [31] try to provide a series of explanations for the peculiar behavior of relaxor ferroelectrics. All these models lead to the formulation of the concept of the origin of dynamic and formation of polar nano-regions.

It is interestingly observed that if the cations in parent compounds are replaced by a small number of foreign ions with different ionic charge and radius, it breaks the long-range ferroelectric polar domains and converts them into many polar islands which are known as polar nanoregions [33, 34]. The formation of PNRs has been related to the appearance of intrinsic inhomogeneity in the material due

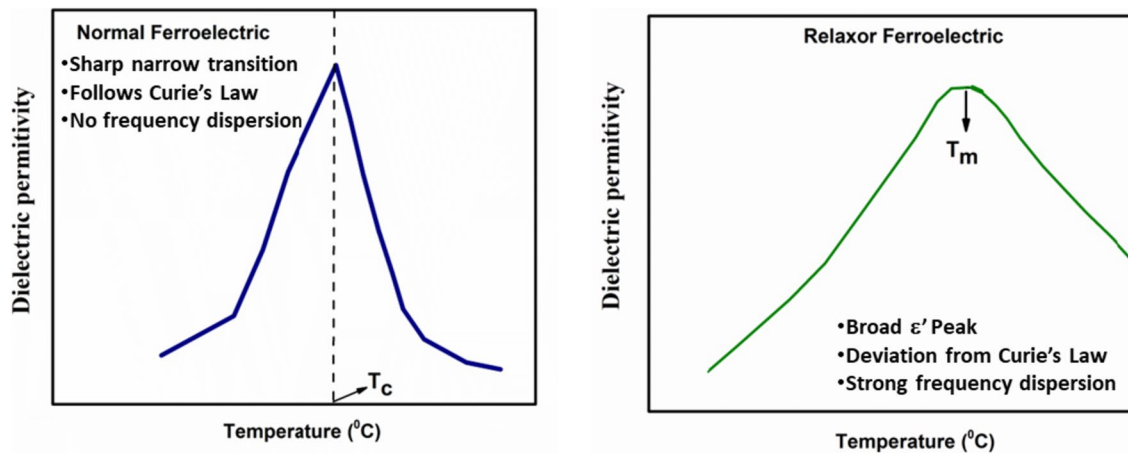


Fig. 7 Temperature-dependent dielectric permittivity for normal and relaxor ferroelectric

to the compositional fluctuations at the crystallographic site and structural modification of the unit cells.

2.3 Dielectric properties

These are the class of insulating materials that get polarized under the effect of the external electric field. In these materials, the electrostatic field can be preserved for a long time. Layers of these materials are used in between the capacitors to enhance the charge storage capacity. Relative permittivity (ϵ_r) or dielectric constant is a measure of the polarization of a material. The higher the permittivity of a material larger the polarization per unit resultant field leads to applications of the electroceramics for engineering and electronic industries [35]. A class of dielectric materials exhibits spontaneous polarization that is polarization of a material even in the absence of any field and this class is known as ferroelectric materials. This property can be induced in a material either by changing composition or by a change in temperature.

2.4 Optical properties

The optical properties of a material are directly related to the shifts in the electronic structures at the fundamental level [36, 37]. With excellent optical and photoluminescence properties, perovskites have provided a promising material for the next generation of solar cells for use in high-performance photovoltaic devices [38]. The advantage of cationic substitutions at either A or B sites can tune their optical and electrical properties. On one hand, ABO_3 semiconductors like $BaTiO_3$ provide an interesting photovoltaic effect caused by excellent ferroelectric properties [39]. On the other hand, recently, investigators have suggested that optical gas sensing platforms caused by oxygen vacancies in $LaMnO_3$ can provide benefits over conventional sensors and have high-temperature applications in combustion environments, due

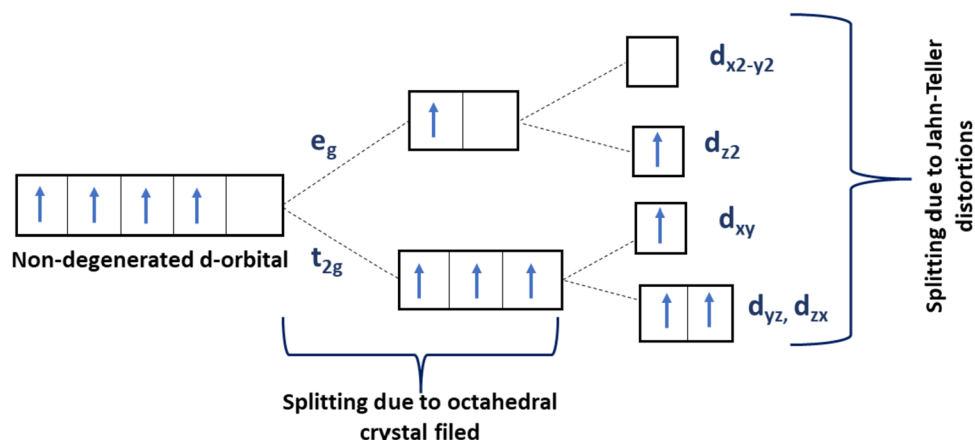
to their high decomposition temperatures and structural stability [40, 41]

2.5 Magnetic properties

The perovskite oxides have special magnetic properties due to the strong electron–electron interaction with the 3d manifold and considerable physical strength [7, 42, 43]. Because of their possible applications as technological magnetic materials, magnetic perovskite oxides have attracted the most attention [43]. One of the most studied classes of perovskite materials for their magnetic behavior is the Manganite perovskite with Mn-ions at the B-site. These compounds show a weak spontaneous magnetic moment, due to slight canting of the B-site ion's moments, which are otherwise antiferromagnetically aligned. Ideally in cubic perovskite structure, each oxygen is shared by two Mn^{3+} ions forming a $[MnO_6]$ octahedron with Mn ion at the central position surrounded by six O ions. The transition metal ion at B-site due to the presence of d-orbital, results in electric crystal field splitting (CFT). The degenerate d orbitals split, due to the octahedral crystal field, into two two-fold degenerate e_g orbitals (d_z^2 and $d_{x^2-y^2}$) higher in energy than three-fold degenerate t_{2g} orbitals (d_{xy} , d_{yz} , and d_{zx}). If one or both t_{2g} and e_g levels are partially occupied, these energy levels further split due to JT distortion as shown in Fig. 8. Under JT distortion, both t_{2g} and e_g levels split, with the same mean energy of each set of levels [7].

The magnetic properties of manganites are explained by the transfer of electrons that occur between the manganese and the oxygen orbitals. The magnetic interactions are mediated by O 2p electrons as the direct overlap between Mn orbitals is small. These magnetic interactions are mediated either by double exchange interaction or by superexchange interaction as discussed below.

Fig. 8 Splitting in d-orbital (of Mn^{3+}) due to octahedral crystal field and Jahn–Teller distortions



2.5.1 Double-exchange interaction

It is a type of magnetic exchange that may arise between ions with different oxidation states (Mn^{3+} and Mn^{4+}). This mechanism predicts the relative ease with which an electron may be exchanged between the two species and has more implications for whether the materials are ferromagnetic, antiferromagnetic, or exhibit spiral mechanisms. The hopping of an electron from Mn^{3+} to Mn^{4+} via oxygen ion where the Mn^{3+} and Mn^{4+} ions exchange takes place [44], or the simultaneous transfer of one electron from an Mn^{3+} 3d e_g orbital to an $\text{O} 2p$ orbital and transfer from the same $\text{O} 2p$ orbital to unoccupied 3d e_g orbital of the Mn^{4+} ion is termed as double-exchange interaction as shown in Fig. 9a.

This exchange of electrons from one ion to another will be facilitated more easily if the electron does not have to change spin direction to confirm Hund's rule. The e_g electron is spin-polarized because of Hund's interaction with its core (t_{2g}). For the hopping of electrons, relative orientation of the spins of the e_g electrons and the "vacant" core is a crucial factor. If the direction of the core spin of the

Mn^{4+} -ion is opposite to that of the e_g electron of the neighboring Mn^{3+} -ion, then hopping is forbidden. This simple picture demonstrates the direct relation between hopping and ferromagnetic (FM) ordering and describes qualitatively the origin of the ferromagnetism in the manganites [7, 44].

2.5.2 Superexchange interactions

For perovskite manganites, FM interactions are not only governed by DE interaction alone but also by the nature of superexchange interactions [42]. If two orbitals of adjacent ions one orbital fully occupied and the other orbital with a vacancy, point towards each other, then the electron will spend part of the time at the empty orbital of the other ion, these types of interactions are termed superexchange interactions [7]. In the case of manganite perovskites, electrons are shared between an occupied $\text{O} 2p$ orbital and a vacant $\text{Mn} e_g$ orbital and can be regarded as a virtual transfer of the electron [7] as shown in Fig. 9b.

Superexchange interaction can be further divided into two classes of exchange interactions between spins of

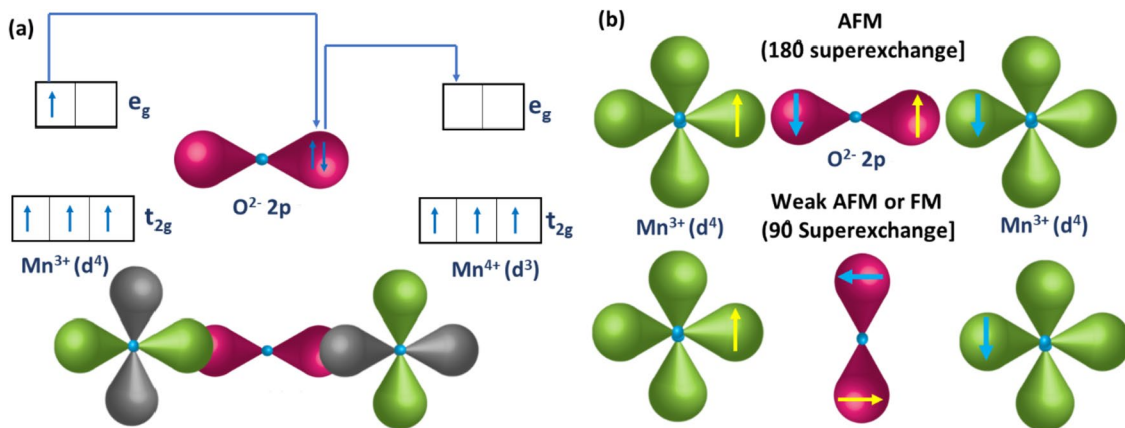


Fig. 9 Schematic diagram of **a** double exchange interaction and **b** superexchange interaction [45]

different atoms: (i) Direct exchange, which occurs between spin moments on atoms with wave functions that are significantly overlapping and decreases rapidly with increasing interatomic distance, and (ii) indirect exchange, where the spin moments are coupled over relatively large distances [44]. Direct exchange intermediate by a nonmagnetic ion is termed a superexchange interaction while indirect exchange intermediate through itinerant electrons is known as Ruderman–Kittel–Kasuya–Yoshida interaction (RKKY). Superexchange interactions generally occur in insulators while RKKY in metals [46–48]. The corresponding superexchange interactions depend on the orbital configuration following the rules of Goodenough–Kanamori. Generally, for $\text{Mn}^{4+}\text{--O--Mn}^{4+}$, the interaction is AFM, whereas for $\text{Mn}^{3+}\text{--O--Mn}^{3+}$, it may be FM or AFM [49].

The perovskite manganites such as LaMnO_3 , CaMnO_3 , PrMnO_3 , and NdMnO_3 are insulators and undergo an antiferromagnetic (AFM) transition at low temperatures. The AFM ordering is of A-type, G-type, and C-type, as shown in Fig. 10. AFM materials, which were initially considered to be not so useful materials, have recently observed a renewed interest due to their potential for technologies such as spintronics, opto-spintronics, THz information technologies, neuromorphic computing, magnetic random-access memory (MRAM) devices, and several other applications [50–52].

2.6 Multiferrocity

Multiferroic materials are a special class of solid compounds in which magnetic, electric, or piezo-elastic phases coexist,

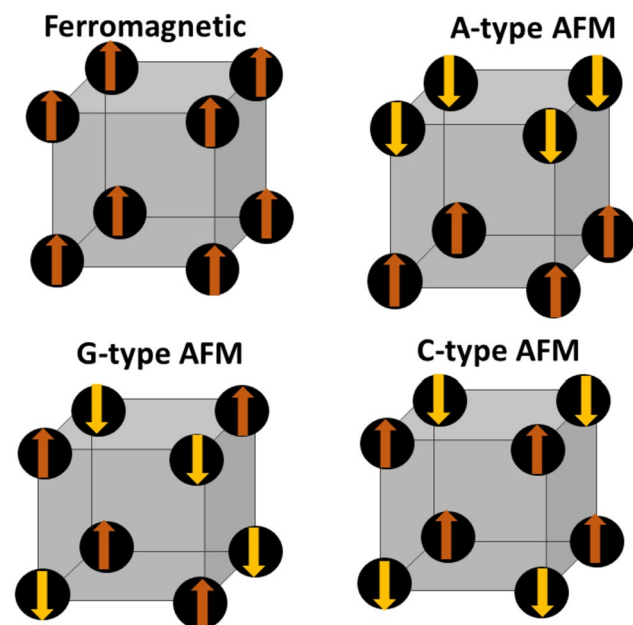


Fig. 10 Schematic representation of different types of magnetic ordering

this means that they have a spontaneous magnetization that can be reoriented by an applied magnetic field, a spontaneous polarization that can be reoriented by an applied electric field, and a spontaneous deformation that can be reoriented by an applied stress. Ferroelectricity and ferromagnetism derive from the fact that the electrons possess charge and spin. The electric charges of electrons and ions are responsible for the charge effects, whereas electron spins govern magnetic properties. Depending on the surroundings, a material may have an electric polarization or a magnetic polarization. A few materials possess both ferroelectric and magnetic polarizations (as shown in Fig. 11) and are called multiferroic [53].

Aside from the fundamental physics of multiferroic materials which is rich and fascinating, these materials are likely to offer a whole range of new applications due to the coupling between ferroelectric and magnetic domains [54]. For example, the ability to couple either electric or magnetic polarization can use the additional degree of freedom in spintronic device applications. Other applications include multiple-state memory elements, in which data is stored both in the electric and magnetic polarizations, and novel memory media, which might allow the writing of a ferroelectric data bit and reading of the magnetic field generated by association [55].

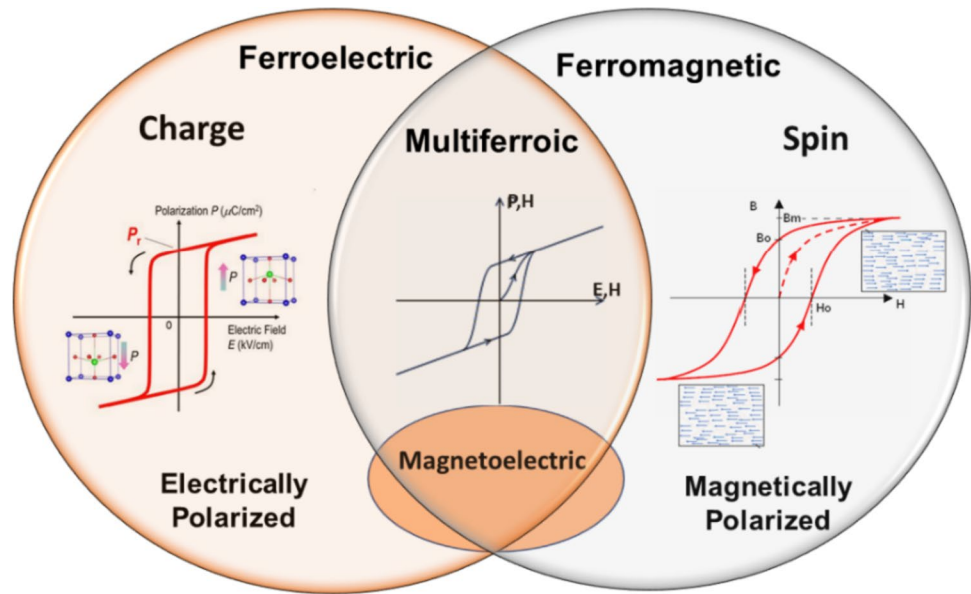
Generally, the multiferroics are divided into two groups. The first group contains those materials in which ferroelectricity and magnetism have different sources and appear largely independently of one another, though there is some coupling between them termed type-I multiferroics. In these materials, ferroelectricity typically appears at higher temperatures than magnetism, and the spontaneous polarization P is often rather large (of order $10 - 100 \mu\text{C}/\text{cm}^2$). The second group, type-II multiferroics, in which magnetism causes ferroelectricity, implies a strong coupling between the two. However, the polarization in these materials is usually much smaller [56].

2.6.1 Requirements for the existence of multiferrocity in a material

(i) Symmetry

A primary requirement for the existence of ferroelectricity is a structural distortion that removes the center of symmetry and allows an electric polarization. However, on the other hand, magnetic properties require a crystal structure with the highest crystal symmetry. Therefore, for the occurrence of magnetic and electric order states in the same phase, strict symmetry conditions must be required. Magnetic ordered crystals with spontaneous magnetization must be invariant under space inversion symmetry operation and crystals with electric order phase permitting a spontaneous

Fig. 11 Multiferroic combining the properties of ferroelectric and ferromagnetic

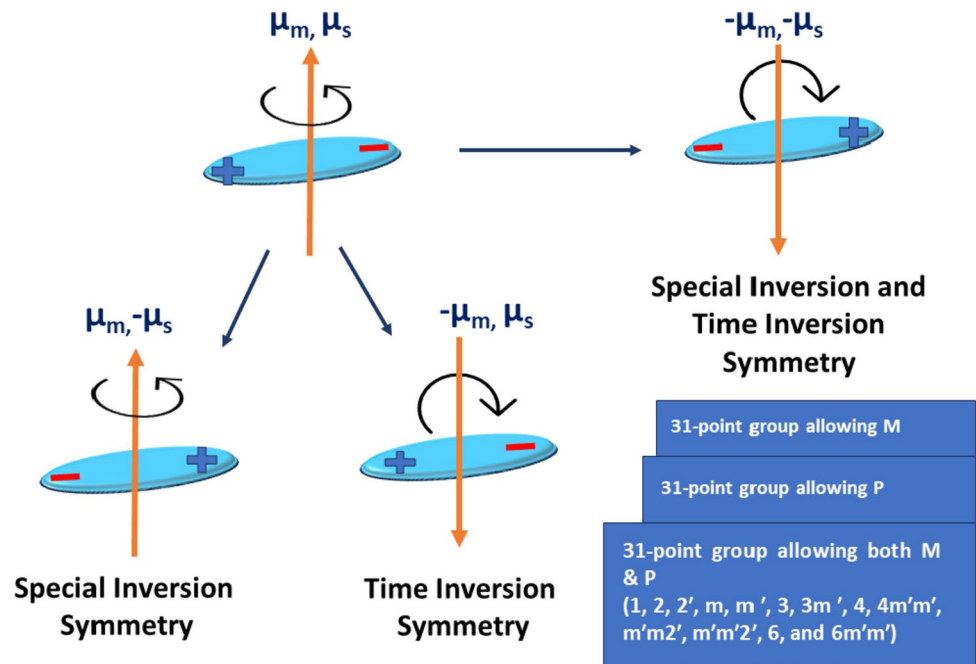


electric polarization must be invariant under time reversal symmetry as shown in Fig. 10 [57]. According to Shubnikov point groups the total number of possible crystal structures is 122 [43]. Out of all 122 possible point groups, 31 crystallographic point groups allow spontaneous polarization P , and 31-point groups allow spontaneous magnetization M [58]. Thirteen crystallographic point groups are found in both sets that allow both electric and magnetic order to coexist in the same phase [57, 59]. The 13 crystallographic point groups allowing multiferroic phase are shown in Fig. 12.

(b) *Electrical properties*

Ferroelectric materials are dielectric insulators that allow the external electric field to polarize the electric dipoles. Although ferromagnetic materials do not require specific electric properties and are generally metals. The high density of state at the Fermi level is the driving force for ferromagnetism which also results in metallicity [58]. Hence, insulating materials with weak ferromagnetic properties such as perovskite manganites have become important for

Fig. 12 Special and time inversion symmetry of multiferroic perovskites



multiferroic applications due to their AFM order and insulating characteristics [7].

(iii) d^0 - d^n scenario

In the case of transition metals, the ferroelectric property is generally driven by d^0 -shell while d-orbitals with unpaired electrons show magnetic behavior. If d-orbital is vacant then there will be no magnetic ordering of any type. However, if the d-orbital is partially occupied, the tendency of distortion in the crystal structure that removes the center of symmetry is eliminated, which results in a lack of ferroelectricity in the material [58, 60]. This is termed a d^0 - d^n dilemma which can be solved in three ways and achieve multiferroicity in perovskite [61].

- Let ferroelectric and ferromagnetic active ions occupy different Wyckoff positions. For example, in BiFeO₃, ferroelectric active cation Bi³⁺ occupies the A-site while magnetic cation Fe³⁺ occupies the B-site of perovskite. Prepare double perovskite in which one of the sublattices is magnetic and the other is ferroelectric.
- Prepare magnetic perovskite in which ferroelectricity is strongly related to spiral magnetic order.

3 Literature review

Examples of selective perovskite materials such as BaTiO₃ (BT), Ba_{0.5}Na_{0.5}TiO₃ (BNT), KNbO₃ (KN), K_{0.5}Na_{0.5}NbO₃ (KNN), BiFeO₃ (BFO), LaMnO₃ (LMO), BaMnO₃ (BMO), LaFeO₃ (LFO), and their doped parts are explained in the following section and are categorized, based on their most studies properties.

3.1 Perovskite materials with electrical properties

Perovskite materials with different electrical properties like ferroelectric and piezoelectric such as BaTiO₃ (BT), BaNaTiO₃ (BNT), KNbO₃ (KN), K_{0.5}Na_{0.5}NbO₃ (KNN), are most widely studied because of their potential electromechanical properties, MPB, high Curie temperature, excellent high-temperature performances, and can be used in high and low-frequency energy harvesting applications. These materials have the potential to replace Lead-based perovskite materials, which makes them fascinating materials for research. However, for the complete replacement of lead-based materials, these materials need to be studied attentionally.

3.1.1 BaTiO₃ and their derivatives

Barium titanate (BT) traced in the 1940s had been the most important piezoelectric material due to its sizable piezoelectric coefficient of about 120–190 pC/N², which is

significantly higher than that of older piezoelectric materials such as triglycine sulfate (TGS), KH₂PO₄ (KDP), quartz, etc. [62]. However, compared with PZT, with an outstanding piezoelectric coefficient of about 350–700 pC/N². Because of its mediocre response in terms of both piezoelectricity and T_c (about 130 °C), BT is used as a high dielectric-constant capacitor for discrete and multi-layer capacitor (MLC) applications [63]. The high dielectric properties of BT are associated with ferroelectricity [64].

BaTiO₃ is a definite chemical compound with highly stable components, synthesis with simple synthesis conditions, and is easy to sinter while maintaining good chemical stoichiometry. To modify and improve the basic properties, BT is not used in its true chemical form but is combined with special additives such as Sr²⁺, Nd²⁺, Ca²⁺, and Co²⁺ [65]. These special additives are selected depending on the use or application of BT. Generally highest dielectric constant values are obtained around T_c; hence, lower T_c is desired, so that the higher dielectric constant values associated with the T_c occur nearer room temperature [25].

Besides its mediocre response in terms of piezoelectricity, in the search for Pb-free material for piezoelectric applications, the researcher has studied Barium titanate as an important piezoelectric material. Composite of BT such as (BaZr)TiO₃-(Ba, Ca)TiO₃ (BZT-BCT), Ba(Sn, Ti)O₃-(Ba, Ca)TiO₃ (BST-BCT) and Ba(Hf, Ti)O₃-(Ba, Ca)TiO₃ (BHT-BZT) are reported to show piezoelectric response comparable to soft PZT ceramics [66–69]. The reason for high piezoelectricity in these BT-based composites is the existence of Morphotropic phase boundaries (MPB) like lead-based perovskite (PZT) [70, 71]. MPB is an interface between two different crystal phases like ferroelectric tetragonal and ferroelectric rhombohedral with the highest dielectric and piezoelectric coefficient around this region.

An important derivative of BT-based perovskite for lead-free piezoelectric material is (BaNa)TiO₃ (BNT) perovskite materials. BNT is traced back to 1960 by Smolenskii and has attracted much attention due to its large remnant polarization (P_r = 38 μC/cm²) [72, 73]. However, due to high conductivity and large coercivity, these materials are poor piezoelectric materials. However, composition modification by ion substitution or solid solutions leads to the formation of phase boundaries, which promote the piezoelectric behavior of these materials [74, 75]. Two types of phase boundaries are observed to be exerted in chemically modified BNT-based materials. The first phase boundary MPB-I is the R-T phase boundary which is related to the piezoelectric response, while the second phase boundary MPB-II is responsible for the maximum strain response of BNT-based materials due to non-polar to polar phase transition [76].

Compositional modification of BNT can be obtained by making binary or ternary BNT-based perovskites. for example (BaNaTiO₃- BaTiO₃)BNT-BT [77, 78], (BaNaTiO₃- BaKTiO₃)

BNT-BKT [79, 80], (BaNaTiO₃-SrTiO₃) BNT-ST [81, 82], (BaNaTiO₃-LiNbO₃) BNT-LNN [83], (BaNaTiO₃-KNaNbO₃) BNT-KNN [84], etc. are binary system that leads morphotropic phase boundary while, (BaNaTiO₃-BaKTiO₃-KNaNbO₃) BNT-BKT-KNN, (BaNaTiO₃-BaTiO₃-KNaNbO₃) BNT-BT-KNN, (BaNaTiO₃-BaTiO₃-BiLiTiO₃) BNT-BT-BLT, (BaNaTiO₃-BaKTiO₃-BiAgTiO₃) BNT-BT-BAT, (BaNaTiO₃-BaTiO₃-BaZrO₃) BNT-BT-BZ etc. are ternary system with two types of phase boundaries. MPB-I can improve the piezoelectric response, while MPB-II can be employed to promote the strain properties of BNT-based materials [85–89]. According to the report of Jo et al., the electric field-induced reversible nonpolar-to-polar phase transition was responsible for the high strain [90]. All these characteristics lead to the application of BNT-based ceramics in actuator applications. Figure 13a illustrates the piezoelectric coefficient of BT-based materials for the last 10 years best to our knowledge.

3.1.2 KNaNbO₃ (KNN) and their derivatives

Discovered in the 1960s, KNN materials are potential candidates for piezoelectric devices because of their high Curie temperature and outstanding electrical properties [91–93]. Potassium niobate (KNbO₃) ceramic shows nearly three times higher longitudinal piezoelectric coefficients along certain non-polar crystallographic directions than the polar axis [94]. It exhibits phase transition from cubic-tetragonal (C-T) at 435 °C, tetragonal-orthorhombic (O-T) at 225 °C, and orthorhombic-rhombohedral (O-R) at -10 °C; however, bulk piezoelectric coefficient of KNbO₃ is low; hence, different dopants are used to modify the piezoelectric properties of KNbO₃.

Compositional modification used to adjust the material properties by inducing the phase boundaries has successfully improved the piezoelectric coefficient (490–570 pC/N) so far [95–97]. It has been reported that by introducing relaxor behavior in addition to the new phase boundary an ultrahigh piezoelectric response (650 ± 20 pC/N) can be obtained [98]. For constructing new phase boundaries, the main strategy involves increasing the R–O phase transition temperature (T_{R-O}) to room temperature while simultaneously decreasing the O–T phase transition temperature (T_{O-T}) to room temperature, in this way, new phase boundaries (i.e., R–T or R–O–T) can be obtained. These phase transitions can be achieved by compositional modification of KNN-based ceramic using special additives such as Li, Bi, Ag, Zr, Hf, and Sb [99–101]. Figure 13b illustrates the piezoelectric coefficient of KNN-based materials for the last 10 years (to the best of our knowledge).

In addition to the piezoelectric effect, other electrical properties including electrocaloric effect (ECE) and energy-storage properties have also been induced in KNN-based ceramics via compositional modification [102, 103]. However, despite of large piezoelectric response of KNN-based ceramics, some challenges still hinder the development of these materials. For example, the highly reactive nature of potassium, the dependence of electrical properties on synthesis conditions such as calcination, and sintering temperature, and the gaps between the properties of the ceramics and device requirements are responsible for the poor piezoelectric performance and failure mechanisms of electronic devices [104].

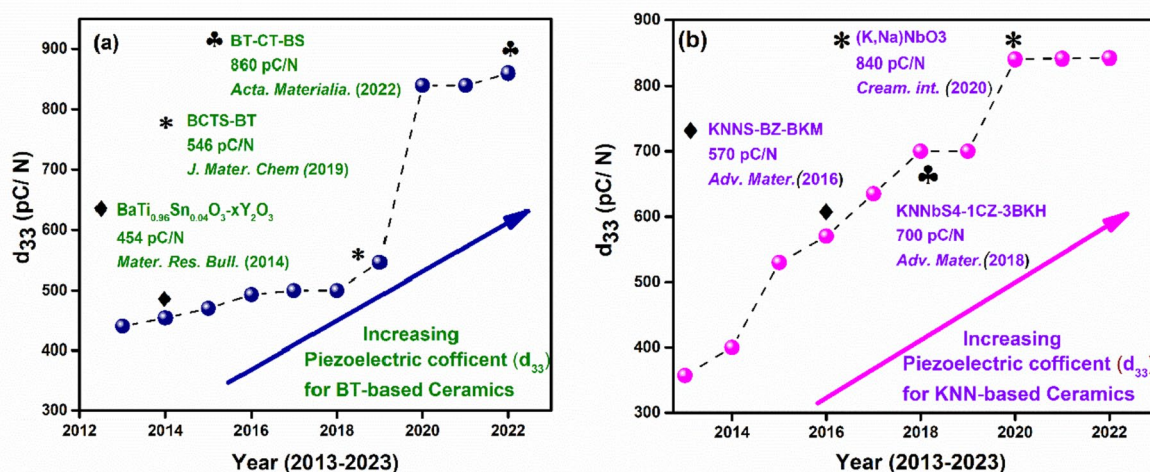


Fig. 13 Evolution of d_{33} in **a** BT and **b** KNN-based ceramics

3.2 Perovskite materials with multiferroic properties

For non-volatile information storage in tapes and hard drives, commonly used materials are ferromagnetic, while ferroelectrics find applications in non-volatile memory devices, where the information stored in the electric polarization is retained, even after removing the power of the device. The simultaneous magnetic and electric order makes it possible for the magnetic polarization to be switched not only by applying a magnetic field but also by an electric field, or likewise, the electric polarization can be switched by applying an electric and/or a magnetic field. This property can be exploited in the generation of completely new devices for a wide range of applications. The following section gives a detailed study of different multiferroic perovskites and their derivatives.

3.2.1 BiFeO₃ (BFO)

The single-phase multiferroic BFO is the only perovskite with room temperature multiferroic order. It is a fully recognized room-temperature multiferroic perovskite with all three ferroic orders. The ferroelectric phase transition temperature (T_c) is around = 1143 K [105], antiferromagnetic order with Neel temperature (T_N) around 643 K [106], and exhibits weak ferromagnetism at room temperature. Ferroelectric order originates from the lone electron pair of Bi³⁺, while magnetic ordering is due to the unpaired Fe spins. BFO is a G-type antiferromagnetic material in which Fe³⁺ ions are surrounded by six neighboring Fe³⁺ ions with spin anti-parallel to the central ion [106]. The canting of the antiferromagnetic sublattices, resulting in a macroscopic magnetization, results in weak ferromagnetism in these materials.

After the discovery of a large ferroelectric polarization (60 $\mu\text{C}/\text{cm}^2$) in thin films of BFO, it became an intense topic of research. The ferroelectric polarizations in bulk BFO are very small compared to thin film and single crystal due to the high conductivity of the samples caused by oxygen vacancies. However, BFO ceramics tend to show polarization values up to 40 $\mu\text{C}/\text{cm}^2$ as reported by Shvartsman et al. [107]. The large polarization up to 120 $\mu\text{C}/\text{cm}^2$ led to a growing interest in BFO thin films, polycrystalline, and ceramics, which has endured until the present day. Despite all the characteristics, BFO devices have major drawbacks due to high leakage current, a tendency to fatigue, and thermal decomposition near the coercive field. These drawbacks can be resolved by appropriate doping.

3.2.2 Manganite perovskites

Manganites are a group of materials exhibiting very interesting magnetoelectric properties. Mostly these materials are insulators with AFM ordering, multiferroic order can be exerted in these materials by appropriate doping. In mixed-valence perovskite manganites $\text{Ln}_{1-x}\text{A}_x\text{MnO}_3$, where Ln is a rare-earth atom such as La, Pr, Nd, and Sm, etc. and A is an alkaline-earth element (like Sr, Ca, and Ba), the application of an external magnetic field, H, strongly enhances the electrical conductivity, resulting in colossal magnetoresistance (CMR) effect.

CMR is an important property of manganese-based perovskite oxides, which enables them to dramatically change the electrical resistance due to magnetic field. Off-centering of Mn-ions, DE interactions, and superexchange interactions are responsible for the CMR effect in these materials. Generally, the CMR effect is closely related to its manganites which are correlated electron systems with the interplay among the lattice spin, charge and orbital degrees of freedom, Jahn-Teller effect, electronic phase separation, charge ordering, etc. The choice of trivalent Ln and divalent A elements in the perovskite A-sites of AMnO_3 perovskite lattice and their ratio can effectively tune different structural and magnetic phases and maintain the balance between competing interactions.

3.2.3 Hexagonal manganites perovskites

Depending on the ionic radius of rare-earth ions, the AMnO_3 systems have two basic structures either hexagonal or orthorhombic. Rare-earth ions at A-site with small ionic radius fall into hexagonal manganites AMnO_3 systems (A = Ho, Er, Tm, Yb, Lu, Y, Sc, and In) are a unique class of materials with multiferroic order in combination with frustrated low-dimensional magnetism on a triangular lattice. They consist of sheets of $[\text{MnO}_5]$ triangular bipyramids connected by $[\text{AO}_7]$ polyhedral. The magnetic ordering is derived from the electronic d^4 configuration of Mn^{3+} on the B-site, and the ferroelectric moment is largely derived from shifts of the A^{3+} in its coordination sphere.

Since the ferroelectric polarization originates from a structural geometry variation, the hexagonal AMnO_3 family is sometimes also classified as geometric ferroelectrics [108]. This ferroelectricity is much stronger than the magnetism-driven ferroelectricity in the perovskite counterparts. Besides the ferroelectricity, one source of magnetism is the Mn^{3+} spins, another source of magnetism may be related to the rare earth A^{3+} 4f spins at very low temperatures. Therefore, the magnetism and ferroelectricity in hexagonal AMnO_3 have different origins independent of each other. However, spin–lattice coupling is available for the

magnetolectric response [106]. Figure 14 represents some important applications of multiferroic materials.

4 Applications of perovskite materials

Perovskite oxide's characteristic of accepting several ions at different sites of crystal structure results in distinct magnetic, electrical, and multiferroic properties as discussed in the above sections. These properties lead to exploit the use of these perovskite oxides in a wide range of applications.

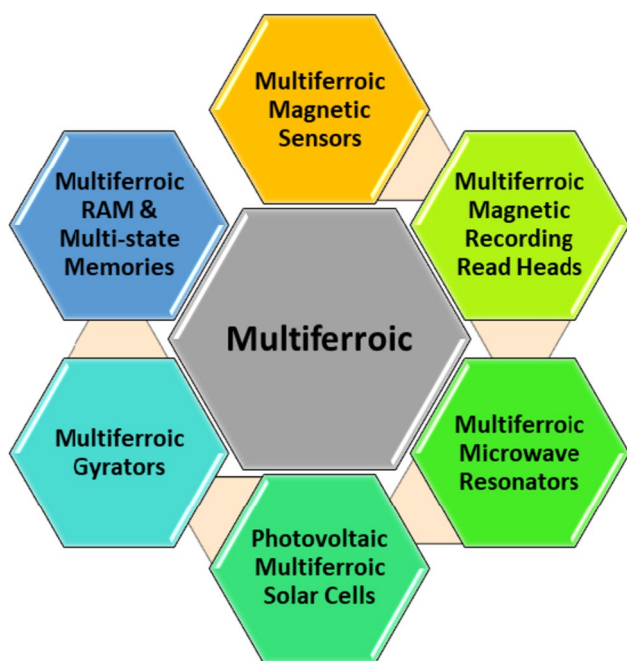


Fig. 14 Applications of multiferroic materials [109–114]

Distinct applications associated with the above-mentioned properties are reviewed in the following section.

4.1 Energy storage applications

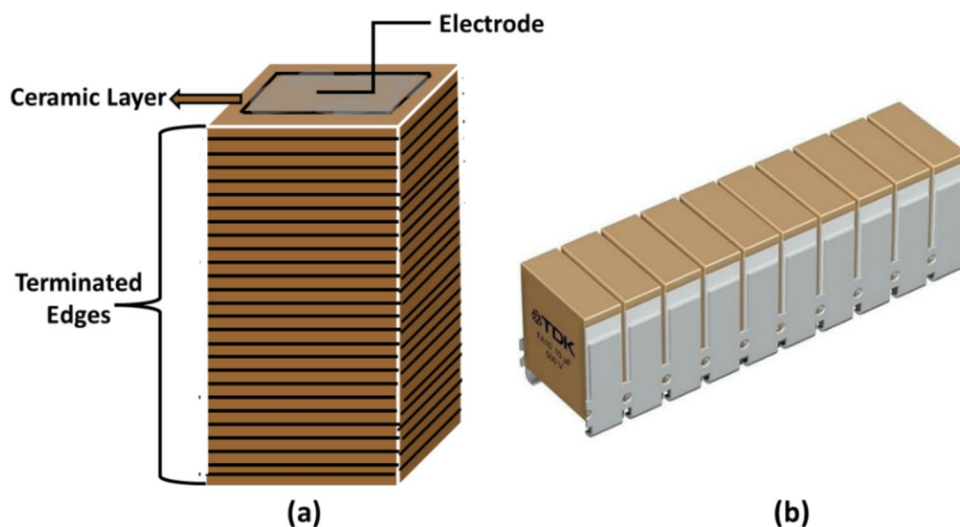
4.1.1 Multi-layer ceramic capacitors (MLCCs)

The dielectric capacitor is an important way to meet the fast increase in the demand for energy storage systems with ultrahigh power density and fast charge–discharge capability. BaTiO₃-based capacitor is considered one of the candidates for MLCCs due to their high permittivity. A capacitor consists of a pair of parallel metal plates separated by free space. When a voltage is applied across these plates, a charge is developed on them proportional to the applied voltage. If an insulating material is placed between the plates, the charge on the plates increases by the relative dielectric permittivity.

A multilayer ceramic capacitor is a capacitor made up of multiple layers of ceramic material as shown in Fig. 15a. MLCCs are effective in enhancing capacitance and reducing capacitor size, highly resistant to abnormal voltage, show high dielectric strength, save energy while they are used in electronic circuits, filter out unwanted noise as part of an audio or radio circuit, and stabilize the voltage level in a circuit. However, one drawback associated with FE materials is that the effective capacitance drops drastically with increasing applied field (<https://www.tdk-electronics.tdk.com/en/1054426/products/product-catalog/ceramic-capacitors/ceralink-capacitors>). Hence, capacitance density is reduced at operating voltage, which constrains certain applications, such as DC-link capacitors.

This drawback has been overcome by antiferroelectric NaNbO₃-based ceramics. Antiferroelectric (AFE) materials are characterized by double polarization hysteresis loops due to the electric-field-induced phase transition from the

Fig. 15 **a** MLCC and **b** commercially available CeraLink capacitor [115]



antiferroelectric (AFE) phase to the ferroelectric (FE) phase [116]. AFE materials are generally characterized by an increase in capacitance with increasing applied field before reaching the critical electric field (E_f) where the AFE-FE phase transition occurs [117, 118].

4.1.2 Supercapacitors

To address the rapid depletion of fossil fuels, the need of today's hour is to identify the resources for sustainable energy sources and new technologies associated with energy conversion and storage. Ubiquitous demand for energy has depleted the natural resources, which is expected to reach 18.30 billion tons of oil equivalent by 2035 and has concentrated the attention of researchers towards the evolution of renewable energy sources [119, 120]. Fuel cells, batteries, and supercapacitors (SCs) are the main energy conversion and energy storage techniques. Among them, SCs have the advantage of rapid charge and discharge kinetics compared to batteries. SCs have the advantages of high-power density, and long cycle life compared to conventional dielectric capacitors [121].

In SCs, there is no dielectric between conducting plates, rather than there is an electrolyte and a thin insulator (separator) between the electrodes. This separator is sandwiched between the electrodes as shown in Fig. 16. SCs can be classified into two categories based on the charge storage mechanism, electrochemical double-layer capacitors (EDLCs) and pseudocapacitors (PCs) [122]. EDLCs store charge through charge accumulation at the interface between the electrolyte and the electrode's surface or a non-faradaic reaction while PCs store charge through a faradaic reaction which is the transfer of charge between the electrode and electrolyte. PCs often show far higher energy density (by a factor of 10 or higher) and capacitance values than EDLCs as the

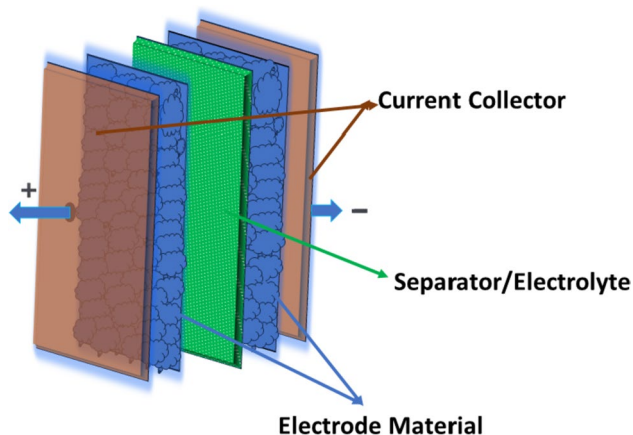


Fig. 16 Different components of SCs

electrochemical reactions occur both on the surface and in the bulk near the solid electrode surface in PCs [123].

Owing to their low cost, robust skeleton structure, high tap density, inherent nature of containing oxygen vacancies, and distinctive chemical tailoring, perovskite oxides have rapidly drawn intensive attention. The advantage of using perovskite oxides over metal oxides is that perovskite oxides do not require a high surface area to achieve high energy storage. The following factors can affect the SC performance using perovskite oxides:

- (i) The compositional flexibility of perovskite oxides brings enormous benefits for SCs. For long cycle-life, structural stability of electrode materials is a very important factor. Hence, to maintain the structural integrity of perovskites, the selection of cations is very crucial. Generally, A-site metal significantly elevates the thermodynamic stability, and B-site metal regulates the electrochemical reactions. For the electrode material applications in SCs, alkaline-earth (such as Sr and Ba) and rare-earth metals (such as La and Sm) are the principal A-site cations, and the B-site cation is usually a transition metal (such as Mn, Co, and Ni) [124]. Some perovskite oxides used in supercapacitors are listed in Table 1.
- (ii) Electrical properties also affect the SCs' performances. Among ABO_3 -type perovskite, the cubic structure has the most effective orbital overlap. If the structure is deviated from cubic with distortion, the degree of overlap decreases and results in reducing conductivity. The low electrical conductivity leads to high consumption of energy during charging/discharging and hence harms the supercapacitor performance [121].
- (iii) Phase transformation in perovskite oxide can be overcome by creating oxygen vacancies in perovskite oxides which result in high oxygen ion mobility, which is responsible for the perovskite's fast kinetic charge storage [124].

4.1.3 Solid-oxide fuel cells (SOFCs)

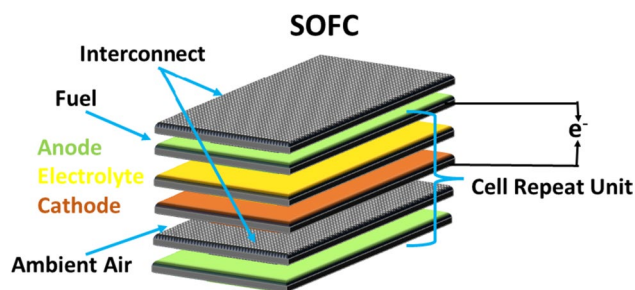
Fuel cells are considered efficient alternatives to combustion engines which minimize the environmental influence of the use of fossil fuels and reduce environmental pollution. Invented over a century ago, these are unique substitutes for ignition engines that can be used in distinct applications such as generating power for satellites and space capsules, powering fuel cell vehicles like automobiles, buses, or boats, and generating primary or emergency backup power for buildings. The basic working principle includes

Table 1 Perovskite oxide-based materials for supercapacitor applications

Composition	Electrolyte	Surface area (m ² g ⁻¹)	Specific capacitance (F g ⁻¹)	Energy density (Wh g ⁻¹)	Ref
La-based perovskites					
LaMnO _{3-x}	6 M KOH	10.6	609	220.4	[125]
LaMnO ₃	1 M KOH	-	520	-	[126]
LaMn _(1-x) O ₃	6 M KOH	35.4	-	-	[127]
LaMnO _{3-x}	6 M KOH	-	937.5	-	[128]
LaMnO ₃	1 M KOH	-	-	-	[129]
LaNiO _{3-x}	6 M KOH	181.2	139.2	65.85	[130]
LaNiO _{3-x}	1 M KOH	-	478.7	-	[131]
LaCrO ₃	3 M LiOH	8.08	24.4	-	[132]
LaNiO _{3-x}	1 M KOH	-	280	-	[133]
LaFeO ₃	2 M KOH	45.09	313.21	-	[134]
LaCoO ₃	6 M KOH	-	706.9	47.64	[135]
LaFeO ₃	1 M Na ₂ SO ₄	41	241.3	34	[136]
La _{1-x} Nd _x NiO ₃	—	-	64.381	20.92	[137]
La _{0.7} Sr _{0.3} NiO _{3-x}	1 M Na ₂ SO ₄	15.46	719	81.4	[138]
La _{0.7} Sr _{0.3} CoO _{3-x}	1 M Na ₂ SO ₄	32.2	747.75	34.8	[139]
La _{0.7} Sr _{0.3} FeO _{3-x}	1 M Na ₂ SO ₄	27.96	523.2	-	[140]
La _{0.2} Sr _{0.8} MnO _{2.7}	1 M KOH	10.5	492	-	[141]
La _{1-x} Sr _x MnO ₃	0.1 KOH	-	-	-	[142]
La _{0.85} Sr _{0.15} MnO ₃	1 M KOH	-	198	3.6	[143]
LaNi _{0.45} Fe _{0.55} O _{3-x}	1 M KOH	10	75	7.5	[144]
La _{0.8} Nd _{0.2} Fe _{0.8} Mn _{0.2} O ₃	3 M KOH	-	158	-	[145]
La _{0.8} Nd _{0.2} Fe _{0.8} Mn _{0.2} O ₃	1 M H ₂ SO ₄	8.16	56.4	1.8	[145]
La _{0.85} Sr _{0.15} Mn _{0.9} Ni _{0.1} O ₃	6 M KOH	-	113.9	-	[146]
La _{0.5} Sr _{0.5} Cu _{0.1} Mn _{0.9} O _{3-x}	1 M Na ₂ SO ₄	30.9	464.5	54.5	[147]
La _{0.75} Sr _{0.25} Cr _{0.5} Mn _{0.5} O ₃	1 M KOH	-	751	-	[148]
Sr-based Perovskite					
SrRuO ₃	1 M KOH	-	52.4	-	[149]
SrTiO ₃	3 M KOH	50.4	590	27.8	[150]
SrCoO ₃	6 M KOH	1.53	572	27.5	[151]
SrMn _{0.8} Co _{0.2} O ₃	½ M Na ₂ SO ₄	-	418	-	[152]
Ba _{0.5} Sr _{0.5} Co _{0.8} Fe _{0.2} O _{3-x}	6 M KOH	0.74	610	-	[151]
SrB _{0.875} Nb _{0.125} O ₃ (B = Mn, Co)	1 M Na ₂ SO ₄	-	894	82.33	[153]

the transformation of chemical energy into electrical energy simply by using a special chemical compound. Out of all fuel cells, SOFCs hold the greatest potential due to their great efficiency, modular and distributed nature, low emissions, zero noise pollution, and low operating cost.

There are many types of fuel cells, with a single common design and process. A negative electrode (an anode) and a positive electrode (a cathode) are sandwiched in an electrolyte and undergo an electrochemical reaction to produce an electric current as shown in Fig. 17. The electrolyte is a conductor that conducts ions either from the fuel to the air or the air to the fuel to create electron flow. The choice of proper materials for SOFCs application is a necessary condition as the chosen material should operate at a high temperature of about 500–800 °C so that cell durability is not compromised.

**Fig. 17** Solid oxide fuel cell (SOFC)

As discussed, perovskite oxides exhibit fascinating properties like high ionic conductivity, good electrical conductivity like metals, and perfect mixed ionic

and electronic conductivity; they are chosen as an effective component in SOFC [154]. $\text{Ba}_{0.5}\text{Sr}_{0.5}\text{Co}_{0.8}\text{Fe}_{0.2}\text{O}_{3-\delta}$, $\text{Ba}_{0.5}\text{Sr}_{0.5}\text{Co}_{0.2}\text{Fe}_{0.8}\text{O}_{3-\delta}$, $\text{La}_{0.7}\text{Sr}_{0.3}\text{Co}_{0.5}\text{Fe}_{0.5}\text{O}_3$, $\text{La}_{0.6}\text{Sr}_{0.4}\text{Fe}_{0.8}\text{Co}_{0.2}\text{O}_3$, NdFeO_3 , $\text{Sm}_{0.5}\text{Sr}_{0.5}\text{CoO}_{3-\delta}$, $\text{La}_{0.75}\text{Sr}_{0.25}\text{Cr}_{0.5}\text{Mn}_{0.5}\text{O}_3$, and $\text{La}_{0.8}\text{Sr}_{0.2}\text{Cr}_{0.9}\text{V}_{0.03}\text{O}_3$ are some perovskite-based materials used as a cathode and anode materials in SOFCs [155–158].

4.2 Piezoelectric energy harvesters

4.2.1 Actuators

A device that is used to convert input energy into mechanical energy is termed an actuator. Piezoelectric actuators possess features such as higher displacement accuracy, higher response speed, and larger generation force compared to electromagnetic, hydraulic, and pneumatic actuators. These features exploited the use of piezoelectric actuators in active damping control, precise positioning, and consumer equipment such as cellular phone terminals and digital cameras. These actuators are also used in industrial equipment that requires precise positioning such as atomic force microscope (AFM) and probes for scanning electron microscope (SEM).

A piezoelectric actuator makes use of the converse piezoelectric effect which makes the piezoelectric coefficient, the defining parameter for non-resonant applications, and mechanical quality factor dominate the resonant piezoelectric actuator applications. The binary and ternary systems like BNT-BT or BNT-BT-KNN have been studied as a piezoelectric material for multilayer ceramic actuators [159], while BNT-BKT-BT ternary systems are reported for cylindrical actuators [160].

4.2.2 Transducers

It is a device that uses piezoelectric material to [161] convert electric, mechanical, or acoustic energy such as sound, water, and kinetic energy into another kind of energy. These are very important devices for detecting natural disasters and underground targets [162]. Piezoelectric transducers are divided according to their working principle. For example, a transducer that converts electrical signals into acoustic signals is known as an electroacoustic transducer. Electroacoustic transducers are used in piezoelectric buzzers, microspeakers, etc. Lead-free KNN and BNT-based materials are suitable for electroacoustic transducer applications.

Another kind of transducer is the ultrasonic transducer that converts electrical signals into sound waves of frequency higher than 20 kHz. These transducers are used in ultrasonic diagnosis techniques which are found to be more effective than X-ray, CT scan, and MRI. Due to the toxic nature of lead-based materials, it is very important to replace these materials with biocompatible materials, especially in

the case of biomedical applications. BFO, BNT, and KNN-based materials are reported to show properties like PZT-based materials and are found promising candidates for low-frequency ultrasonic transducers [66, 69].

4.2.3 Sensors

To detect different acoustic pressure, piezoelectric sensors are used that generate electric signals when a physical strain is applied. These sensors are being used to detect the speed of the car, detect the vibration of structures [163], inspect gas leaks in the environment [164], and examine the human body in the medical domain [165]. These are the piezoelectric energy harvesters (PEH) that operate in non-resonant or resonant conditions. For non-resonant operating conditions, piezoelectric materials should possess high piezoelectric (d) and voltage coefficients (g), while for the sensor to operate near resonance, piezoelectric materials should possess a high coupling constant (k) and mechanical quality factor (Q_m). Because of their high piezoelectric coefficients, KNN and BT-based materials are often employed to fabricate PEH. The sensors based on these materials exhibit the same level of output voltage as that fabricated with PZT and are currently available in the market [166].

Acoustic emission sensors have also attracted a lot of attention as they transform elastic wave acoustic emission (AE) into an electrical signal. A sudden deformation induced by stress can generate a transient elastic wave, which is called acoustic emission (AE). Like PEH sensors, high piezoelectric coefficients are important parameters to fabricate these sensors. Both hard and soft KNN-based ceramics are used to fabricate acoustic emission sensors [167]. For example, a resonator fabricated by lead-free $\text{K}_{0.475}\text{Na}_{0.475}\text{Li}_{0.05}(\text{Nb}_{0.92}\text{Ta}_{0.05}\text{Sb}_{0.03})\text{O}_3$ ceramics for acoustic energy harvesting was reported in 2017 [168]. Some piezoelectric energy harvesting applications are illustrated in Fig. 18.

4.3 Spintronics

In the twenty-first century, developing high-speed information technology is urgently needed. New methodologies such as nanoelectronics, molecular electronics, spintronics, and quantum information techniques have been proposed; among these, spintronics is the promising one as it is compatible with conventional techniques. These conventional electronics can be directly extended to spintronics, the only difference is that conventional techniques use electron's charge while spintronics incorporates electron spin as an active element for processing, data storage, and transfer as shown in Fig. 19. Spintronics is a new independent field in condensed matter physics devoted to investigating the spin-dependent

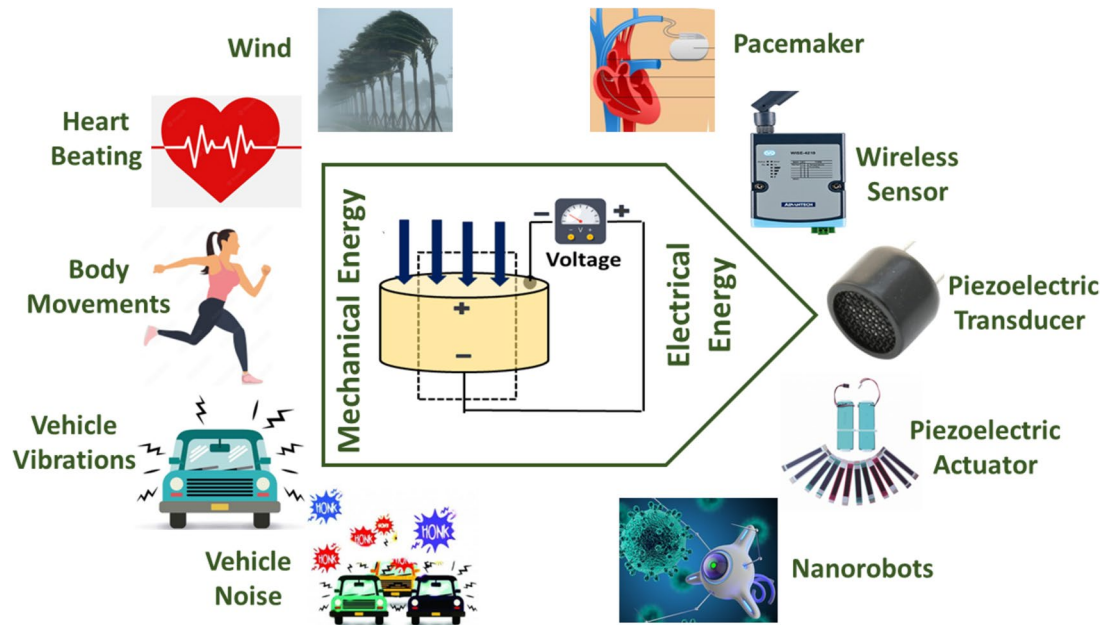
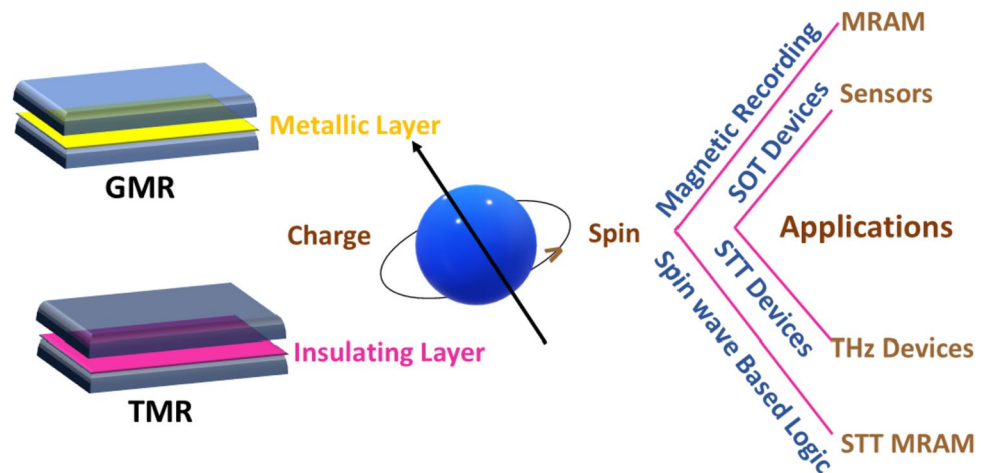


Fig. 18 Piezoelectric energy harvesting applications

Fig. 19 Spintronic device applications



electron transport in solids and low-dimensional structures [169].

The discovery of giant magnetoresistance (GMR) is considered the beginning of spintronics and currently, GMR and tunnel magnetoresistance (TMR) are the two unique phenomena attracting most of the attention of researchers.

(i) Giant magnetoresistance (GMR)

In multilayer magnetic structures, external magnetic field is used to control the magnetic state of a multilayer nanostructure, which provides the control of a polarized current through it. It consists of two layers of ferromagnetic metals sandwiching one layer of non-magnetic metal, when the

magnetization directions in the two ferromagnetic metals are made parallel or antiparallel to each other by applying an external magnetic field, the conductivity across the device differs by an order of magnitude [170]. A large conductivity difference can be obtained by replacing the middle layer with a non-magnetic insulator. The well-known applications of GMR now are magnetoresistive random-access memory, and magnetic field sensors used to read data in hard disk drives.

(b) Tunnel magnetoresistance (TMR)

TMR is another spintronics effect that has given rise to many experimental and theoretical studies. The tunnel magnetoresistance (TMR) in magnetic tunnel junctions (MTJs)

has been known since the experiments of Julliere [171]. Like a GMR device, an MTJ consists of two ferromagnetic metallic electrodes sandwiching a very thin insulating barrier so that the carriers must cross by quantum–mechanical tunneling. If a bias voltage is applied across the electrodes of this junction, a current flows through it, the current intensity being determined by the electron structure of the electrodes and the characteristics of the potential barrier formed by the dielectric layer [10]. It is like a GMR device; the only difference is the separating material in GMR is metallic while for TMR the separating material is a very thin insulating material so that the carriers can tunnel through the separating layer.

4.3.1 Choice of materials for spintronic device applications

Materials with high magnetic ordering temperature (at least higher than room temperature) and large spin polarization around the Fermi energy level are preferred for practical spintronic device applications [170]. In the century of device miniaturization, multifunctional materials that can perform more than one task by external stimuli provide tremendous advantages for spintronics by bringing additional functionalities. Perovskite oxides with tuneable properties such as ferroelectricity, ferromagnetism, antiferromagnetism, metallicity, superconductivity, and optical properties are considered as most versatile material so far [10]. Manganite perovskite materials due to their high spin polarization, high temperature of transition to the ferromagnetic state, and well-developed fabrication technology of thin manganite films particularly in multilayer structures are the most studied materials for spintronics applications [169]. In mixed-valence manganite such as $\text{La}_{1/2}\text{Sr}_{1/2}\text{MnO}_3$ (LSMO) with SrTiO_3 barrier (LSMO/STO/LSMO), TMR of 83% was found at 4.2 K [172] which was increased to 450% in LSMO/STO/LSMO junction at 4.2 K [173]. The half-metallic character of LSMO contributes to 95% spin polarization corresponding to the TMR effect [174]. Multiferroic materials such as BiFeO_3 and BiMnO_3 are widely studied for barriers or spin filters [175, 176].

Antiferromagnetic materials have great potential and are being deployed to reduce device power consumption and scale, which makes them outstanding candidates for the next generation of spintronic applications. Ultimately, antiferromagnets could replace ferromagnets as the active spin-dependent element on which spintronic devices are based. Through their ultrafast dynamics, robustness against perturbation due to magnetic fields, absence of production of parasitic stray fields, and generation of large magneto-transport effects AFM materials have several interesting properties [177]. Antiferromagnets, ferrimagnets, or helical magnets have zero or small magnetization and often an intriguingly complex magnetic structure. These materials

are more common than ferromagnets and can be metals, superconductors, semimetals, semiconductors, or insulators, in comparison to the primarily metallic ferromagnets [52]. Another appealing property of antiferromagnets is the orders of magnitude faster spin-dynamics time scale than in ferromagnets. The antiferromagnetic resonance is in THz, driven by the strong exchange interaction between the spin sublattices, while the GHz ferromagnetic resonance is governed by the weak anisotropy energy.

The recent experimental achievements in AFM materials, such as spin–orbit torque (SOT), spin pumping, anisotropic magnetoresistance, anomalous Hall effect, and spin Seebeck effect, hold up the promises for future outstanding developments [178, 179]. A particularly thrilling aspect of AFM materials is their wide variety in nature. Despite all these advancements, significant challenges such as a better understanding of the SOT mechanism to enhance switching efficiency, and voltage control still need to be thoroughly addressed before antiferromagnets can become active elements of real spintronic devices [52, 177, 178, 180]. The magnetic texture of antiferromagnets is greatly sensitive to the layer thickness, temperature, and growth conditions; the impact of the magnetic on the spin transport properties remains to be accurately understood [181, 182]. Despite the recently rapidly growing literature on AFM spintronics, the field is still in its infancy and it is difficult to predict the future course of basic research in the field and viable applications.

5 Practical examples where perovskite materials are applicable

- The market of multilayer ceramic capacitors (MLCCs) is estimated to be 9 billion \$ in 2018, with a total annual consumption of about 4.5 trillion units of MLCCs globally [183].
- The CeraLink capacitor (TDK EPCOS) is at present the only commercially-available product based on AFE materials as shown in Fig. 10b [116].
- The global market for supercapacitors is estimated to be worth \$25 billion by 2030. GODI India, a Hyderabad-headquartered lithium-ion cell manufacturer, has developed what it calls India’s first-ever 3000F high-power supercapacitors meant for electric vehicle (EV) and renewable energy storage system (ESS) applications.
- In the current study, published in “ACS Energy Letters,” the researchers from IISc’s Department of Instrumentation and Applied Physics (IAP) fabricated their supercapacitor using “Field Effect Transistors” or FETs as the charge collectors, instead of the metallic electrodes that are used in existing capacitors.

- Supercapacitors are exploited in various electric vehicles one such example is the Tata Magic hybrid. It is the prototype with the conventional battery pack with SCs.
- The global SOFC market was estimated to be worth \$1.5 billion in 2020 and is poised to reach \$6.5 billion by 2027. Some examples of commercially available SOFCs are SOFC APU, Delphi SOFC, PureCell Model 400 Bloom Energy Server “BloomBox” etc.
- Researchers from Spain’s Public University of Navarra and Rey Juan Carlos University have used perovskites to create lossy mode resonance (LMR) devices, which are devices that act like super-sensitive detectors that can pick up even the slightest changes in their environment. The key to making LMR devices work is choosing the right material for a thin film. Perovskites have unique properties that allow them to generate LMRs, which are like “sweet spots” where the material especially interacts with light. These sweet spots can be fine-tuned by adjusting the thickness of the perovskite film, among other parameters.
- Researchers at Nanjing University and the University of Illinois at Urbana-Champaign have drawn inspiration from the enhanced visual system of the Papilio Xuthus butterfly and developed an imaging sensor capable of “seeing” into the UV range inaccessible to human eyes. The design of the sensor uses stacked photodiodes and perovskite nanocrystals (PNCs) capable of imaging different wavelengths in the UV range. Using the spectral signatures of biomedical markers, such as amino acids, this new imaging technology is even capable of differentiating between cancer cells and normal cells with 99% confidence.
- Researchers at the Indian Institute of Science Education and Research (IISER) have developed new LEDs that emit light simultaneously in two different wavelength ranges, for a simpler and more comprehensive way to monitor the freshness of fruit and vegetables. The team explains that modifying the LEDs with perovskite materials causes them to emit in both the near-infrared range and the visible range, a significant development in the contact-free monitoring of food. Angshuman Nag and his team at the Indian Institute of Science Education and Research (IISER) are proposing a perovskite application in LED technology that could simplify the quality control of fresh fruit and vegetables.

6 Conclusions and future perspectives

Perovskite oxide has a unique crystal structure and based on A or B-site occupancy, it has the potential to be exploited in various applications. Deviation from the ideal cubic structure induces different important properties in the perovskite

material due to reduced crystal symmetry. The review aims to provide a brief overview of piezoelectric, dielectric, ferroelectric, relaxor ferroelectric, magnetic, and multiferroic properties of selected perovskite oxides such as BiFeO₃, LaMnO₃, LaFeO₃, BaMnO₃, KNN, BT, and BNT along with their associated energy storage applications using MLCCs, supercapacitors, SOFCs, and piezoelectric harvesters. These properties are highly dependent on the non-stoichiometry of anions or cations, the valance state of electronic structure, distortion in the perovskite structure, and the mixed valance state which has also been discussed in this review.

Energy harvesting and energy storage are the two main concerns to overcome energy crises and perovskite materials have the potential to provide both. Electrical, chemical, and dielectric properties of perovskite materials are exploited in energy storage applications by MLCCs, SCs, and SOFCs. Different prototypes of these devices have also been commercialized and are utilized for energy storage applications; however, there are still many perovskite materials that are under intense research to overcome various cons related to these materials. Choice of dopant ions, compositional flexibility, and phase transformation are some constraints that inhibit the use of perovskite materials for energy storage applications.

Despite of long-life, high power density, short charging time and large discharging time, and environmentally friendly properties of supercapacitors, the main disadvantage is that it has low cell voltage. To achieve higher voltages, multiple cells are placed in series, and then it results in the risk of overvoltage, and a DC/DC power converter is required to level the terminal voltage to meet the requirements of applications. These problems can be solved by voltage balance technology and load leveling technology, which need to be studied more intensely. Similarly, to enhance the performance of electrode materials in SCs B-site doping with a transition metal or non-metal still needs to be considered. To boost the electrochemical performance of SCs, the morphology of perovskite oxides and electrolytes plays a crucial role. Therefore, controllable synthesis of nanostructure and use of a redox electrolyte is vital for achieving high power densities and still need to be considered in the design of perovskite oxide electrode materials in the future. Graphene combined perovskite oxides, surface carbon coating modification, and composite with metal oxide like β -MnO₂ can lead to achieving the characteristics of low cost, high specific capacitance, high energy density, and environment friendliness.

BT, BNT, KNN, and their composites are lead-free perovskite materials that can successfully be employed in piezoelectric energy harvesting and energy storage applications. Generally, materials exploited for energy harvesting applications are prone to spread around the environment and have little chance of being collected and recycled afterward,

which implies that these devices should go into production only using lead-free materials. KNN-based high-frequency transducers, a high-frequency linear-array transducers, are examples of devices developed for specific applications. BNT-based piezoelectric ceramics in the ultrasonic cleaner have already been marketed. There are currently many reports available on a prototype of Pb-free piezoelectric devices and materials.

Even though Pb-free piezoelectric materials exhibit unique properties, some constraints such as temperature instability, large hysteresis, low Curie temperature, intrinsic characteristics of phase boundary, and origin of high piezoelectricity limit their capability to replace Pb-based materials completely. Temperature-dependent phase boundaries or “morphotropic phase boundaries (MPB)” and low Curie temperature limit the use of perovskite materials in a broad temperature range. Large hysteresis caused by domain wall motion, and high driving electric field results in insufficient piezoelectric and ferroelectric properties. For larger-scale applications, good comprehensive performance and stability must be achieved. Choice of dopant ions, compositional flexibility, and phase transformation are some constraints that inhibit the use of perovskite materials for energy storage applications. Ongoing experiments on composition modification and phase engineering to balance temperature sensitivity, and defect engineering to promote balance between strain and hysteresis have turned out to be very beneficial so far [184–187]. Further research and accumulated knowledge of perovskite oxide will be beneficial in finding solutions to these issues.

Despite the great potential advantages of spintronics, it now faces several challenges, such as injection of spin into devices, generation of fully spin-polarized carriers, manipulation and detection of carriers’ spin orientation, and long-distance spin transport. The solutions to these issues rely on either the development of device fabrication and optimization techniques or the design of new spintronics materials with specific properties. Although many efforts have been made, obtaining 100% spin-polarized carriers at room temperature remains a challenging job. To date, several research are available in which ferromagnets the main active component of spintronic devices are replaced by an antiferromagnetic material due to its abundance, zero or nearly zero magnetization, and fast switching between different states of antiferromagnets. Antiferromagnets do not create redundant magnetic fields and interact weakly with each other due to zero or nearly zero magnetization, which is particularly important at the nanoscale. However, its complex behavior compared to ferromagnets has not been fully understood yet, which constrains its use in spintronic device applications. To improve the understanding and comprehension of antiferromagnetic spintronics, lots of work is still needed both from theoretical and experimental aspects.

Author contribution Priyanka Thakur: Software, Visualization, Writing-original draft. Navdeep Sharma: Software, Resources, Writing-review & editing. Dinesh Pathak: Writing-review & editing. Pankaj Sharma: Writing-review & editing. Kamal Kishore: Writing-review & editing. Shashi Dhar: Writing-original draft. Madan Lal: Writing-original draft, Conceptualization, data curation, supervision, Writing-review & editing.

Data availability The data of this study will be made available from the corresponding author upon reasonable request.

Declarations

Ethical approval Not applicable.

Conflict of interest The authors declare no competing interests.

References

1. M. Farghali, A.I. Osman, I.M. Mohamed, Z. Chen, L. Chen, I. Ihara, P.S. Yap, D.W. Rooney, Strategies to save energy in the context of the energy crisis: a review. *Environ. Chem. Lett.* **21**, 1–37 (2023)
2. C. Kenny, M. Snyder, Meeting the sustainable development goal zero targets: what could we do?. Center for global development working paper (472) (2017)
3. P.P. Walsh, E. Murphy, D. Horan, The role of science, technology and innovation in the UN 2030 agenda. *Technol. Forecast. Soc. Chang.* **154**, 119957 (2020)
4. S.H. Ali, The materials science imperative in meeting the sustainable development goals. *Nat. Mater.* **17**(12), 1052–1053 (2018)
5. M.I.A. Abdel Maksoud, A.G. Bedir, M. Bekhit, M.M. Abouelela, R.A. Fahim, A.S. Awed, D.W. Rooney, MoS₂-based nanocomposites: synthesis, structure, and applications in water remediation and energy storage: a review. *Environ. Chem. Lett.* **19**, 3645–3681 (2021)
6. M. Telychko, J. Lu, Recent advances in atomic imaging of organic-inorganic hybrid perovskites. *Nano Mater. Sci.* **1**(4), 260–267 (2019)
7. V. Markovich, A. Wisniewski, H. Szymczak, Magnetic properties of perovskite manganites and their modifications. In *Handbook of Magnetic Materials*, vol 22 (Elsevier, 2014), pp. 1–201
8. R.M. Ormerod, Solid oxide fuel cells. *Chem. Soc. Rev.* **32**(1), 17–28 (2003)
9. M.E. Arroyo-de Dompablo, A. Ponrouch, P. Johansson, M.R. Palacín, Achievements, challenges, and prospects of calcium batteries. *Chem. Rev.* **120**(14), 6331–6357 (2019)
10. M. Bibes, A. Barthelemy, Oxide spintronics. *IEEE Trans. Electron Devices* **54**(5), 1003–1023 (2007)
11. A. Barman, S. Kar-Narayan, D. Mukherjee, Caloric effects in perovskite oxides. *Adv. Mater. Interfaces* **6**(15), 1900291 (2019)
12. E.A. Lombardo, M.A. Ulla, Perovskite oxides in catalysis: past, present and future. *Res. Chem. Intermed.* **24**, 581–592 (1998)
13. T. Wolfram, S. Ellialtioglu, *Electronic and optical properties of d-band perovskites* (Cambridge University Press, 2006)
14. Y. Chen, L. Zhang, Y. Zhang, H. Gao, H. Yan, Large-area perovskite solar cells—a review of recent progress and issues. *RSC Adv.* **8**(19), 10489–10508 (2018)
15. K.W. Tan, D.T. Moore, M. Saliba, H. Sai, L.A. Estroff, T. Hanrath, U. Wiesner, Thermally induced structural evolution and performance of mesoporous block copolymer-directed alumina perovskite solar cells. *ACS Nano* **8**(5), 4730–4739 (2014)

16. M.A. Peña, J.L.G. Fierro, Chemical structures and performance of perovskite oxides. *Chem. Rev.* **101**(7), 1981–2018 (2001)
17. N.F. Atta, A. Galal, E.H. El-Ads, Perovskite nanomaterials—synthesis, characterization, and applications. *Perovskite materials—synthesis, characterisation, properties, and applications.* (2016), pp. 107–151
18. T. Jia, Z. Zeng, X. Zhang, P. Ohodnicki, B. Chorpeneing, G. Hackett, Y. Duan, The influence of oxygen vacancy on the electronic and optical properties of ABO_{3-δ} (A= La, Sr, B= Fe, Co) perovskites. *Phys. Chem. Chem. Phys.* **21**(36), 20454–20462 (2019)
19. F.S. Galasso, *Structure, properties and preparation of perovskite-type compounds: international series of monographs in solid state physics*, vol. 5 (Elsevier, 2013)
20. L.Q. Jiang, J.K. Guo, H.B. Liu, M. Zhu, X. Zhou, P. Wu, C.H. Li, Prediction of lattice constant in cubic perovskites. *J. Phys. Chem. Solids* **67**(7), 1531–1536 (2006)
21. H. Huang, L. Polavarapu, J.A. Sichert, A.S. Sussha, A.S. Urban, A.L. Rogach, Colloidal lead halide perovskite nanocrystals: synthesis, optical properties and applications. *NPG Asia Mater.* **8**(11), e328–e328 (2016)
22. C.G. Bischak, C.L. Hetherington, H. Wu, S. Aloni, D.F. Ogletree, D.T. Limmer, N.S. Ginsberg, Origin of reversible photoinduced phase separation in hybrid perovskites. *Nano Lett.* **17**(2), 1028–1033 (2017)
23. T. Kleckner, A.I. 1-Electrical strain gauges, piezoelectric sensors or fiberbragg sensors for force measurement: prospects and potentials. *Proc. Sens.* **2013**, 23–27 (2013)
24. V. Raghavan, *Materials science and engineering: a first course.* PHI Learning Pvt Ltd (2015)
25. <https://resources.pcb.cadence.com/blog/2020-understanding-a-ferroelectric-hysteresis-loop-in-electronics> (open link)
26. G.H. Haertling, Ferroelectric ceramics: history and technology. *J. Am. Ceram. Soc.* **82**(4), 797–818 (1999)
27. Y. Xu, *Ferroelectric materials and their applications* (Elsevier, 2013)
28. O. Auciello, J.F. Scott, R. Ramesh, The physics of ferroelectric memories. *Phys. Today* **51**(7), 22–27 (1998)
29. F. Jona, G. Shirane, Ferroelectric crystals. (1962)
30. M.D. Nguyen, C.T. Nguyen, H.N. Vu, G. Rijnders, Experimental evidence of breakdown strength and its effect on energy-storage performance in normal and relaxor ferroelectric films. *Curr. Appl. Phys.* **19**(9), 1040–1045 (2019)
31. C.W. Ahn, C.H. Hong, B.Y. Choi, H.P. Kim, H.S. Han, Y. Hwang, I.W. Kim, A brief review on relaxor ferroelectrics and selected issues in lead-free relaxors. *J. Korean Phys. Soc.* **68**, 1481–1494 (2016)
32. L.K. Pradhan, M. Kar Relaxor ferroelectric oxides: concept to applications. *Multifunctional ferroelectric materials.* (2021), pp. 49
33. Z. Yang, F. Gao, H. Du, L. Jin, L. Yan, Q. Hu, Y.J. Wang, Grain size engineered lead-free ceramics with both large energy storage density and ultrahigh mechanical properties. *Nano Energy* **58**, 768–777 (2019)
34. F. Li, J. Zhai, B. Shen, H. Zeng, Recent progress of ecofriendly perovskite-type dielectric ceramics for energy storage applications. *J. Adv. Dielectr.* **8**(06), 1830005 (2018)
35. S.F. Hoeffler, G. Trimmel, T. Rath, Progress on lead-free metal halide perovskites for photovoltaic applications: a review. *Monatsh. Chemie-Chem. Monthly* **148**, 795–826 (2017)
36. Y. Jia, A. Miglio, X. Gonze, M. Mikami, Ab-initio study of oxygen vacancy stability in bulk and Cerium-doped lutetium oxyorthosilicate. *J. Lumin.* **204**, 499–505 (2018)
37. L. Dong, R. Jia, B. Xin, B. Peng, Y. Zhang, Effects of oxygen vacancies on the structural and optical properties of β-Ga₂O₃. *Sci. Rep.* **7**(1), 40160 (2017)
38. N.A. Noor, Q. Mahmood, M. Rashid, B.U. Haq, A. Laref, S.A. Ahmad, Ab-initio study of thermodynamic stability, thermoelectric and optical properties of perovskites ATiO₃ (A= Pb, Sn). *J. Solid State Chem.* **263**, 115–122 (2018)
39. S. Dahbi, N. Tahiri, O. El Bounagui, H. Ez-Zahraouy, Electronic, optical, and thermoelectric properties of perovskite BaTiO₃ compound under the effect of compressive strain. *Chem. Phys.* **544**, 111105 (2021)
40. J. Park, Y.N. Wu, W.A. Saidi, B. Chorpeneing, Y. Duan, First-principles exploration of oxygen vacancy impact on electronic and optical properties of ABO_{3-δ} (A= La, Sr; B= Cr, Mn) perovskites. *Phys. Chem. Chem. Phys.* **22**(46), 27163–27172 (2020)
41. Y. Jee, J.K. Wuenschell, H.W. Abernathy, S. Lee, T.L. Kalapos, G.A. Hackett, P.R. Ohodnicki, High-temperature oxygen sensing behavior of perovskite films on the optical fiber platform. In *Oxide-based Materials and Devices X*, vol 10919 (SPIE, 2019), pp. 233–241
42. J.B. Goodenough, Metallic oxides. *Prog. Solid State Chem.* **5**, 145–399 (1971)
43. L.K. Aminov, B.Z. Malkin, M.A. Teplov, *Handbook of the Physics and Chemistry of Rare Earths*, vol. 22, ed. by K.A. Gschneider Jr., L. Eyring (2002)
44. A.K. Kundu, Magnetic perovskites. *Eng. Mater.* (2016)
45. C.L. Prajapat, S. Singh, D. Bhattacharya, G. Ravikumar, S. Basu, S. Mattauach, A. Paul, Proximity effects across oxide-interfaces of superconductor-insulator-ferromagnet hybrid heterostructure. *Sci. Rep.* **8**(1), 3732 (2018)
46. H.U. Habermeyer, G. Cristiani, R.K. Kremer, O. Lebedev, G. Van Tendeloo, Cuprate/manganite superlattices: A model system for a bulk ferromagnetic superconductor. *Phys. C: Supercond. Appl.* **364**, 298–304 (2001)
47. C. Zener, Interaction between the d shells in the transition metals. *Phys. Rev.* **81**(3), 440 (1951)
48. A.J. Millis, Electron-lattice coupling in “colossal” magnetoresistance rare earth manganites. *J. Appl. Phys.* **81**(8), 5502–5503 (1997)
49. J.B. Goodenough, Theory of the role of covalence in the perovskite-type manganites [La, M (II)] Mn O₃. *Phys. Rev.* **100**(2), 564 (1955)
50. W. Chen, Z. Sun, Z. Wang, L. Gu, X. Xu, S. Wu, C. Gao, Direct observation of van der Waals stacking-dependent interlayer magnetism. *Science* **366**(6468), 983–987 (2019)
51. P. Němec, M. Fiebig, T. Kampfrath, A.V. Kimel, Antiferromagnetic opto-spintronics. *Nat. Phys.* **14**(3), 229–241 (2018)
52. T. Jungwirth, X. Marti, P. Wadley, J. Wunderlich, Antiferromagnetic spintronics. *Nat. Nanotechnol.* **11**(3), 231–241 (2016)
53. H. Schmid, Multi-ferroic magnetoelectrics. *Ferroelectrics* **162**(1), 317–338 (1994)
54. M. Fiebig, Revival of the magnetoelectric effect. *J. Phys. D Appl. Phys.* **38**(8), R123 (2005)
55. W. Prellier, M.P. Singh, P. Murugavel, The single-phase multi-ferroic oxides: from bulk to thin film. *J. Phys. Condens. Matter* **17**(30), R803 (2005)
56. D. Khomskii, Classifying multiferroics: mechanisms and effects. *Physics* **2**, 20 (2009)
57. M.M. Vopson, Fundamentals of multiferroic materials and their possible applications. *Crit. Rev. Solid State Mater. Sci.* **40**(4), 223–250 (2015)
58. N.A. Hill, Why are there so few magnetic ferroelectrics? *J. Phys. Chem. B* **104**(29), 6694–6709 (2000)
59. L.A. Shuvalov, N.V. Belov, The symmetry of crystals in which ferromagnetic and ferroelectric properties appear simultaneously. *Kristallografiya* **7**(192), 150–151 (1962)
60. N.A. Hill, Density functional studies of multiferroic magnetoelectrics. *Annu. Rev. Mater. Res.* **32**(1), 1–37 (2002)

61. H. Liu, X. Yang, A brief review on perovskite multiferroics. *Ferroelectrics* **507**(1), 69–85 (2017)
62. M. Acosta, N. Novak, V. Rojas, S. Patel, R. Vaish, J. Koruza, G.A. Rossetti, J.J. Rödel, BaTiO₃-based piezoelectrics: fundamentals, current status, and perspectives. *Appl. Phys. Rev.* **4**(4) (2017)
63. J. Gao, X. Ke, M. Acosta, J. Glaum, X. Ren, High piezoelectricity by multiphase coexisting point: barium titanate derivatives. *MRS Bull.* **43**(8), 595–599 (2018)
64. S.I. Shkuratov, C.S. Lynch, A review of ferroelectric materials for high power devices. *J. Materiomics* **8**(4), 739–752 (2022)
65. Z. Yao, H. Liu, Y. Liu, Z. Wu, Z. Shen, Y. Liu, M. Cao, Structure and dielectric behavior of Nd-doped BaTiO₃ perovskites. *Mater. Chem. Phys.* **109**(2–3), 475–481 (2008)
66. L. Zhao, B.P. Zhang, P.F. Zhou, L.F. Zhu, J.F. Li, Effect of Li₂O addition on sintering and piezoelectric properties of (Ba, Ca)(Ti, Sn) O₃ lead-free piezoceramics. *J. Eur. Ceram. Soc.* **35**(2), 533–540 (2015)
67. L.F. Zhu, B.P. Zhang, X.K. Zhao, L. Zhao, F.Z. Yao, X. Han, P.F. Zhou, J.F. Li, Phase transition and high piezoelectricity in (Ba, Ca)(Ti_{1-x}Snx) O₃ lead-free ceramics. *Appl. Phys. Lett.* **103**(7) (2013)
68. C. Zhou, W. Liu, D. Xue, X. Ren, H. Bao, J. Gao, L. Zhang, Triple-point-type morphotropic phase boundary based large piezoelectric Pb-free material—Ba (Ti_{0.8}Hf_{0.2}) O₃-(Ba_{0.7}Ca_{0.3}) TiO₃. *Appl. Phys. Lett.* **100**(22) (2012)
69. D. Xue, Y. Zhou, H. Bao, J. Gao, C. Zhou, X. Ren, Large piezoelectric effect in Pb-free Ba (Ti, Sn) O_{3-x} (Ba, ca) TiO₃ ceramics. *Appl. Phys. Lett.* **99**(12) (2011)
70. W. Wang, L.D. Wang, W.L. Li, D. Xu, Y.F. Hou, W.P. Cao, W.D. Fei, Piezoelectric properties of BaTiO₃-CaTiO₃-BaZrO₃ ceramics with compositions near the morphotropic phase boundary. *Ceram. Int.* **40**(9), 14907–14912 (2014)
71. M. Acosta, N. Novak, G.A. Rossetti, J. Rödel, Mechanisms of electromechanical response in (1-x) Ba (Zr_{0.2}Ti_{0.8}) O_{3-x} (Ba_{0.7}Ca_{0.3}) TiO₃ ceramics. *Appl. Phys. Lett.* **107**(14) (2015)
72. G.A. Smolenskii, A.I. Agranovskaya, S.N. Popov, V.A. Isupov, New ferroelectrics of complex composition. *Sov. Phys. Tech. Phys.* **28**, 2152 (1958)
73. T. Zheng, J. Wu, D. Xiao, J. Zhu, Recent development in lead-free perovskite piezoelectric bulk materials. *Prog. Mater. Sci.* **98**, 552–624 (2018)
74. M. Naderer, T. Kainz, D. Schütz, K. Reichmann, The influence of Ti-nonstoichiometry in Bi_{0.5}Na_{0.5}TiO₃. *J. Eur. Ceram. Soc.* **34**(3), 663–667 (2014)
75. Y.S. Sung, J.M. Kim, J.H. Cho, T.K. Song, M.H. Kim, T.G. Park, Effects of Bi nonstoichiometry in (Bi_{0.5+x}Na) TiO₃ ceramics. *Appl. Phys. Lett.* **98**(1) (2011)
76. S.T. Zhang, A.B. Kouna, E. Aulbach, H. Ehrenberg, J. Rödel, Giant strain in lead-free piezoceramics Bi_{0.5}Na_{0.5}TiO₃-BaTiO₃-K_{0.5}NbO₃ system. *Appl. Phys. Lett.* **91**(11) (2007)
77. S. Ullah Jan, A. Zeb, S.J. Milne, Electrical properties of Ca-modified Na_{0.5}Bi_{0.5}TiO₃-BaTiO₃ ceramics. *Ceram. Int. Int.* **40**(10), 15439–15445 (2014)
78. B. Parija, Morphotropic Phase boundary in BNT-BZT solid solution: a study by Raman spectroscopy and electromechanical parameters. *J. Ceram. Process. Res.* **16**(5), 565–571 (2015)
79. A. Moosavi, M.A. Bahrevar, A.R. Aghaei, P. Ramos, M. Algueró, H. Amorín, High-field electromechanical response of Bi_{0.5}Na_{0.5}TiO₃-Bi_{0.5}K_{0.5}TiO₃ across its morphotropic phase boundary. *J. Phys. D Appl. Phys.* **47**(5), 055304 (2014)
80. Y.R. Zhang, J.F. Li, B.P. Zhang, C.E. Peng, Piezoelectric and ferroelectric properties of Bi-compensated (Bi_{1/2}Na_{1/2}) TiO₃-(Bi_{1/2}K_{1/2}) TiO₃ lead-free piezoelectric ceramics. *J. Appl. Phys.* **103**(7) (2008)
81. H.L. Li, Q. Liu, J.J. Zhou, K. Wang, J.F. Li, H. Liu, J.Z. Fang, Grain size dependent electrostrain in Bi_{1/2}Na_{1/2}TiO₃-SrTiO₃ incipient piezoceramics. *J. Eur. Ceram. Soc.* **36**(11), 2849–2853 (2016)
82. F. Weyland, M. Acosta, J. Koruza, P. Breckner, J. Rödel, N. Novak, Criticality: concept to enhance the piezoelectric and electrocaloric properties of ferroelectrics. *Adv. Func. Mater.* **26**(40), 7326–7333 (2016)
83. T. Chen, T. Zhang, G. Wang, J. Zhou, J. Zhang, Y. Liu, Effect of Li_{0.12}Na_{0.88}NbO₃ content on the electrical properties of Bi_{0.5}Na_{0.5}TiO₃ lead-free piezoelectric ceramics. *J. Alloy. Compd.* **520**, 7–10 (2012)
84. A.B. Kouna, S.T. Zhang, W. Jo, T. Granzow, J. Rödel, Morphotropic phase boundary in (1-x) Bi_{0.5}Na_{0.5}TiO_{3-x}K_{0.5}Na_{0.5}NbO₃ lead-free piezoceramics. *Appl. Phys. Lett.* **92**(22) (2008)
85. D. Lin, K.W. Kwok, H.L.W. Chan, Structure and electrical properties of Bi_{0.5}Na_{0.5}TiO₃-BaTiO₃-Bi_{0.5}Li_{0.5}TiO₃ lead-free piezoelectric ceramics. *Solid State Ionics* **178**(37–38), 1930–1937 (2008)
86. L. Wu, D. Xiao, F. Zhou, Y. Teng, Y. Li, Microstructure, ferroelectric, and piezoelectric properties of (1-x-y) Bi_{0.5}Na_{0.5}TiO_{3-x}BaTiO_{3-y}Bi_{0.5}Ag_{0.5}TiO₃ lead-free ceramics. *J. Alloys Compd.* **509**(2), 466–470 (2011)
87. J. Chen, Y. Wang, Y. Zhang, Y. Yang, R. Jin, Giant electric field-induced strain at room temperature in LiNbO₃-doped 0.94 (Bi_{0.5}Na_{0.5}) TiO₃-0.06 BaTiO₃. *J. Eur. Ceram. Soc.* **37**(6), 2365–2371 (2017)
88. A. Maqbool, A. Hussain, J.U. Rahman, T.K. Song, W.J. Kim, J. Lee, M.H. Kim, Enhanced electric field-induced strain and ferroelectric behavior of (Bi_{0.5}Na_{0.5}) TiO₃-BaTiO₃-SrZrO₃ lead-free ceramics. *Ceram. Int.* **40**(8), 11905–11914 (2014)
89. Y.J. Dai, S. Zhang, T.R. Shrout, X.W. Zhang, Piezoelectric and ferroelectric properties of Li-doped (Bi_{0.5}Na_{0.5}) TiO₃-(Bi_{0.5}K_{0.5}) TiO₃-BaTiO₃ lead-free piezoelectric ceramics. *J. Am. Ceram. Soc.* **93**(4), 1108–1113 (2010)
90. W. Jo, T. Granzow, E. Aulbach, J. Rödel, D. Damjanovic, Origin of the large strain response in (K_{0.5}Na_{0.5}) NbO₃-modified (Bi_{0.5}Na_{0.5}) TiO₃-BaTiO₃ lead-free piezoceramics. *J. Appl. Phys.* **105**(9) (2009)
91. J. Wu, D. Xiao, J. Zhu, Potassium-sodium niobate lead-free piezoelectric materials: past, present, and future of phase boundaries. *Chem. Rev.* **115**(7), 2559–2595 (2015)
92. J. Wu, *Advances in lead-free piezoelectric materials* (Springer, Singapore, 2018), pp.379–396
93. X. Lv, J. Zhu, D. Xiao, X.X. Zhang, J. Wu, Emerging new phase boundary in potassium sodium-niobate based ceramics. *Chem. Soc. Rev.* **49**(3), 671–707 (2020)
94. K. Nakamura, Y. Kawamura, Orientation dependence of electromechanical coupling factors in KNbO₃/sub 3. *IEEE Trans. Ultrason. Ferroelectr. Freq. Control* **47**(3), 750–755 (2000)
95. F. Rubio-Marcos, J.F. Fernandez, D.A. Ochoa, J.E. García, R.E. Rojas-Hernandez, M. Castro, L. Ramajo, Understanding the piezoelectric properties in potassium-sodium niobate-based lead-free piezoceramics: Interrelationship between intrinsic and extrinsic factors. *J. Eur. Ceram. Soc.* **37**(11), 3501–3509 (2017)
96. F. Rubio-Marcos, R. Lopez-Juarez, R.E. Rojas-Hernandez, A. del Campo, N. Razo-Perez, J.F. Fernandez, Lead-free piezoceramics: revealing the role of the rhombohedral-tetragonal phase coexistence in enhancement of the piezoelectric properties. *ACS Appl. Mater. Interfaces* **7**(41), 23080–23088 (2015)
97. B. Wu, H. Wu, J. Wu, D. Xiao, J. Zhu, S.J. Pennycook, Giant piezoelectricity and high Curie temperature in nanostructured alkali niobate lead-free piezoceramics through phase coexistence. *J. Am. Chem. Soc.* **138**(47), 15459–15464 (2016)
98. H. Tao, H. Wu, Y. Liu, Y. Zhang, J. Wu, F. Li, S.J. Pennycook, Ultrahigh performance in lead-free piezoceramics utilizing a

- relaxor slush polar state with multiphase coexistence. *J. Am. Chem. Soc.* **141**(35), 13987–13994 (2019)
99. J. Wu, D. Xiao, Y. Wang, W. Wu, B. Zhang, J. Zhu, Q. Li, Microstructure and electrical properties of (Li, Ag, Ta, Sb)-modified (K_{0.50}Na_{0.50})NbO₃ lead-free ceramics with good temperature stability. *J. Phys. D Appl. Phys.* **41**(12), 125405 (2008)
 100. J. Hao, W. Bai, B. Shen, J. Zhai, Improved piezoelectric properties of (K_xNa_{1-x})_{0.94}Li_{0.06}NbO₃ lead-free ceramics fabricated by combining two-step sintering. *J. Alloy. Compd.* **534**, 13–19 (2012)
 101. P. Palei, P. Kumar, Dielectric, ferroelectric and piezoelectric properties of (1-x)[K_{0.5}Na_{0.5}NbO₃]-x[LiSbO₃] ceramics. *J. Phys. Chem. Solids* **73**(7), 827–833 (2012)
 102. T. Shao, H. Du, H. Ma, S. Qu, J. Wang, J. Wang, Z. Xu, Potassium–sodium niobate based lead-free ceramics: novel electrical energy storage materials. *J. Mater. Chem. A* **5**(2), 554–563 (2017)
 103. S.L. Yang, C.C. Tsai, Y.C. Liou, C.S. Hong, B.J. Li, S.Y. Chu, Investigation of CuO-doped NKN ceramics with high mechanical quality factor synthesized by a B-site oxide precursor method. *J. Am. Ceram. Soc.* **95**(3), 1011–1017 (2012)
 104. J. Wu, Perovskite lead-free piezoelectric ceramics. *J. Appl. Phys.* **127**(19) (2020)
 105. A.J.C. Buurma, G.R. Blake, T.T.M. Palstra, U. Adem, Multiferroic materials: physics and properties. Reference Module in materials science and materials engineering, (2016)
 106. S. Dong, J.M. Liu, S.W. Cheong, Z. Ren, Multiferroic materials and magnetoelectric physics: symmetry, entanglement, excitation, and topology. *Adv. Phys.* **64**(5–6), 519–626 (2015)
 107. V.V. Shvartsman, W. Kleemann, R. Haumont, J. Kreisel, Large bulk polarization and regular domain structure in ceramic BiFeO₃. *Appl. Phys. Lett.* **90**(17) (2007)
 108. S.W. Cheong, M. Mostovoy, Multiferroics: a magnetic twist for ferroelectricity. *Nat. Mater.* **6**(1), 13–20 (2007)
 109. S. Bhuktare, A. Bose, H. Singh, A.A. Tulapurkar, Gyrotor based on magneto-elastic coupling at a ferromagnetic/piezoelectric interface. *Sci. Rep.* **7**(1), 840 (2017)
 110. S. Kumar, P. Kumar, R. Walia, V. Verma, Improved ferroelectric, magnetic and photovoltaic properties of Pr doped multiferroic bismuth ferrites for photovoltaic application. *Results Phys.* **14**, 102403 (2019)
 111. W. Kleemann, Magnetoelectric spintronics. *J. Appl. Phys.* **114**(2) (2013)
 112. A. Moser, K. Takano, D.T. Margulies, M. Albrecht, Y. Sonobe, Y. Ikeda, E.E. Fullerton, Magnetic recording: advancing into the future. *J. Phys. D Appl. Phys.* **35**(19), R157 (2002)
 113. M. Balinskiy, A.C. Chavez, A. Barra, H. Chiang, G.P. Carman, A. Khitun, Magnetoelectric spin wave modulator based on synthetic multiferroic structure. *Sci. Rep.* **8**(1), 10867 (2018)
 114. M.J. Bauer, X. Wen, P. Tiwari, D.P. Arnold, J.S. Andrew, Magnetic field sensors using arrays of electrospun magnetoelectric Janus nanowires. *Microsyst. Nanoeng.* **4**(1), 37 (2018)
 115. G.R. Love, Energy storage in ceramic dielectrics. *J. Am. Ceram. Soc.* **73**(2), 323–328 (1990)
 116. L. Fulanović, M.H. Zhang, Y. Fu, J. Koruza, J. Rödel, NaNbO₃-based antiferroelectric multilayer ceramic capacitors for energy storage applications. *J. Eur. Ceram. Soc.* **41**(11), 5519–5525 (2021)
 117. G.F. Engel, Design and materials of antiferroelectric capacitors for high density power electronic applications. In CIPS 2016; 9th International conference on integrated power electronics systems, (VDE, 2016), pp. 1–7
 118. J. Gao, L. Zhao, Q. Liu, X. Wang, S. Zhang, J.F. Li, Antiferroelectric-ferroelectric phase transition in lead-free AgNbO₃ ceramics for energy storage applications. *J. Am. Ceram. Soc.* **101**(12), 5443–5450 (2018)
 119. S. Chu, Y. Cui, N. Liu, The path towards sustainable energy. *Nat. Mater.* **16**(1), 16–22 (2017)
 120. S. Singh, S. Jain, P.S. Venkateswaran, A.K. Tiwari, M.R. Nouni, J.K. Pandey, S. Goel, Hydrogen: a sustainable fuel for future of the transport sector. *Renew. Sustain. Energy Rev.* **51**, 623–633 (2015)
 121. A.K. Tomar, A. Joshi, G. Singh, R.K. Sharma, Perovskite oxides as supercapacitive electrode: properties, design and recent advances. *Coord. Chem. Rev.* **431**, 213680 (2021)
 122. J. Yan, S. Li, B. Lan, Y. Wu, P.S. Lee, Rational design of nanostructured electrode materials toward multifunctional supercapacitors. *Adv. Func. Mater.* **30**(2), 1902564 (2020)
 123. Y. Liu, Z. Wang, Y. Zhong, X. Xu, J.P.M. Veder, M.R. Rowles, Z. Shao, Activation-free supercapacitor electrode based on surface-modified Sr₂CoMo_{1-x}Ni_xO_{6-δ} perovskite. *Chem. Eng. J.* **390**, 124645 (2020)
 124. Y. Cao, J. Liang, X. Li, L. Yue, Q. Liu, S. Lu, X. Sun, Recent advances in perovskite oxides as electrode materials for supercapacitors. *Chem. Commun.* **57**(19), 2343–2355 (2021)
 125. J.T. Mefford, W.G. Hardin, S. Dai, K.P. Johnston, K.J. Stevenson, Anion charge storage through oxygen intercalation in LaMnO₃ perovskite pseudocapacitor electrodes. *Nat. Mater.* **13**(7), 726–732 (2014)
 126. P.M. Shafi, N. Joseph, A. Thirumurugan, A.C. Bose, Enhanced electrochemical performances of agglomeration-free LaMnO₃ perovskite nanoparticles and achieving high energy and power densities with symmetric supercapacitor design. *Chem. Eng. J.* **338**, 147–156 (2018)
 127. Z.A. Elsiddig, H. Xu, D. Wang, W. Zhang, X. Guo, Y. Zhang, J. Chen, Modulating Mn⁴⁺ ions and oxygen vacancies in non-stoichiometric LaMnO₃ perovskite by a facile sol-gel method as high-performance supercapacitor electrodes. *Electrochim. Acta* **253**, 422–429 (2017)
 128. Y.L. Song, Z.C. Wang, Y.D. Yan, M.L. Zhang, G.L. Wang, T.Q. Yin, ... M. Qiu, Molten salt synthesis and supercapacitor properties of oxygen-vacancy LaMnO_{3-δ}. *J. Energy Chem.* **43**, 173–181 (2020)
 129. V.S. Devi, K. Kannadasan, P.C. Sharafudeen, P. Elumalai, Performance of sodium-ion supercapattery using LaMnO₃ and rGO in non-aqueous electrolyte. *New J. Chem.* **46**(31), 15130–15144 (2022)
 130. Z. Li, W. Zhang, H. Wang, B. Yang, Two-dimensional perovskite LaNiO₃ nanosheets with hierarchical porous structure for high-rate capacitive energy storage. *Electrochim. Acta* **258**, 561–570 (2017)
 131. W. Che, M. Wei, Z. Sang, Y. Ou, Y. Liu, J. Liu, Perovskite LaNiO_{3-δ} oxide as an anion-intercalated pseudocapacitor electrode. *J. Alloy. Compd.* **731**, 381–388 (2018)
 132. N. Arjun, G.T. Pan, T.C. Yang, The exploration of Lanthanum based perovskites and their complementary electrolytes for the supercapacitor applications. *Results Phys.* **7**, 920–926 (2017)
 133. K.H. Ho, J. Wang, Hydrazine reduction of LaNiO₃ for active materials in supercapacitors. *J. Am. Ceram. Soc.* **100**(10), 4629–4637 (2017)
 134. Z. Li, W. Zhang, C. Yuan, Y. Su, Controlled synthesis of perovskite lanthanum ferrite nanotubes with excellent electrochemical properties. *RSC Adv.* **7**(21), 12931–12937 (2017)
 135. G. Guo, K. Ouyang, J. Yu, Y. Liu, S. Feng, M. Wei, Facile synthesis of LaCoO₃ with a high oxygen vacancy concentration by the plasma etching technique for high-performance oxygen ion intercalation pseudocapacitors. *ACS Appl. Energy Mater.* **3**(1), 300–308 (2019)
 136. Y. Zhang, J. Ding, W. Xu, M. Wang, R. Shao, Y. Sun, B. Lin, Mesoporous LaFeO₃ perovskite derived from MOF gel for all-solid-state symmetric supercapacitors. *Chem. Eng. J.* **386**, 124030 (2020)

137. A. Qayyum, M.O. urRehman, F. Ahmad, M.A. Khan, S.M. Ramay, S. Atiq, Performance optimization of Nd-doped LaNiO₃ as an electrode material in supercapacitors. *Solid State Ionics* **395**, 116227 (2023)
138. Y. Cao, B. Lin, Y. Sun, H. Yang, X. Zhang, Sr-doped lanthanum nickelate nanofibers for high energy density supercapacitors. *Electrochim. Acta* **174**, 41–50 (2015)
139. Y. Cao, B. Lin, Y. Sun, H. Yang, X. Zhang, Symmetric/asymmetric supercapacitor based on the perovskite-type lanthanum cobaltate nanofibers with Sr-SUBSTITUTION. *Electrochim. Acta* **178**, 398–406 (2015)
140. W. Wang, B. Lin, H. Zhang, Y. Sun, X. Zhang, H. Yang, Synthesis, morphology and electrochemical performances of perovskite-type oxide La_xSr_{1-x}FeO₃ nanofibers prepared by electrospinning. *J. Phys. Chem. Solids* **124**, 144–150 (2019)
141. C.T. Alexander, J.T. Mefford, J. Saunders, R.P. Forslund, K.P. Johnston, K.J. Stevenson, Anion-based pseudocapacitance of the perovskite library La_{1-x}Sr_xBO_{3-δ} (B= Fe, Mn, Co). *ACS Appl. Mater. Interfaces* **11**(5), 5084–5094 (2019)
142. W. Wang, W. Liu, M. Kamiko, S. Yagi, Enhanced catalytic activity of perovskite La_{1-x}Sr_xMnO_{3+δ} for the oxygen reduction reaction. *New J. Chem.* **46**(27), 13082–13088 (2022)
143. X.W. Wang, Q.Q. Zhu, X.E. Wang, H.C. Zhang, J.J. Zhang, L.F. Wang, Structural and electrochemical properties of La_{0.85}Sr_{0.15}MnO₃ powder as an electrode material for supercapacitor. *J. Alloy. Compd.* **675**, 195–200 (2016)
144. C.T. Alexander, R.P. Forslund, K.P. Johnston, K.J. Stevenson, Tuning redox transitions via the inductive effect in LaNi_{1-x}Fe_xO_{3-δ} perovskites for high-power asymmetric and symmetric pseudocapacitors. *ACS Appl. Energy Mater.* **2**(9), 6558–6568 (2019)
145. A. Rezaezhad, E. Rezaei, L.S. Ghadimi, A. Hajalilou, E. Abouzari-Lotf, N. Arsalani, Outstanding supercapacitor performance of Nd–Mn co-doped perovskite LaFeO₃@ nitrogen-doped graphene oxide nanocomposites. *Electrochim. Acta* **335**, 135699 (2020)
146. P.P. Ma, B. Zhu, N. Lei, Y.K. Liu, B. Yu, Q.L. Lu, G.H. Jiang, Effect of Sr substitution on structure and electrochemical properties of perovskite-type LaMnO₃. *Mater. Lett.* **252**, 23–26 (2019)
147. Y. Cao, B. Lin, Y. Sun, H. Yang, X. Zhang, Synthesis, structure and electrochemical properties of lanthanum manganese nanofibers doped with Sr and Cu. *J. Alloy. Compd.* **638**, 204–213 (2015)
148. Z.U. Rehman, M.A. Raza, A. Tariq, U.N. Chishti, M.F. Maqsood, N. Lee, A. Inam, La_{0.75}Sr_{0.25}Cr_{0.5}Mn_{0.5}O₃ perovskite developed for supercapacitor applications. *J. Energy Storage* **32**, 101951 (2020)
149. A. Galal, H.K. Hassan, T. Jacob, N.F. Atta, Enhancing the specific capacitance of SrRuO₃ and reduced graphene oxide in NaNO₃, H₃PO₄ and KOH electrolytes. *Electrochim. Acta* **260**, 738–747 (2018)
150. A.K. Tomar, G. Singh, R.K. Sharma, Charge storage characteristics of mesoporous strontium titanate perovskite aqueous as well as flexible solid-state supercapacitor cell. *J. Power. Sources* **426**, 223–232 (2019)
151. Y. Liu, J. Dinh, M.O. Tade, Z. Shao, Design of perovskite oxides as anion-intercalation-type electrodes for supercapacitors: cation leaching effect. *ACS Appl. Mater. Interfaces* **8**(36), 23774–23783 (2016)
152. G. George, S.L. Jackson, C.Q. Luo, D. Fang, D. Luo, D. Hu, Z. Luo, Effect of doping on the performance of high-crystalline SrMnO₃ perovskite nanofibers as a supercapacitor electrode. *Ceram. Int.* **44**(17), 21982–21992 (2018)
153. N. Lei, P. Ma, B. Yu, S. Li, J. Dai, G. Jiang, Anion-intercalated supercapacitor electrode based on perovskite-type SrB_{0.875}Nb_{0.125}O₃ (B= Mn, Co). *Chem. Eng. J.* **421**, 127790 (2021)
154. J.T.S. Irvine, Perovskite oxide anodes for SOFCs. Perovskite oxide for solid oxide fuel cells, (2009), pp. 167–182
155. J.M. Tarascon, M. Armand, Materials for sustainable energy: a collection of peer-reviewed research and review articles from Nature Publishing Group. World Scientific **414**, 171–179 (2011)
156. K.W. Song, K.T. Lee, Characterization of Ba_{0.5}Sr_{0.5}M_{1-x}Fe_xO_{3-δ} (M= Co and Cu) perovskite oxide cathode materials for intermediate temperature solid oxide fuel cells. *Ceram. Int.* **38**(6), 5123–5131 (2012)
157. C.H.E.N. Tongyun, S.H.E.N. Liming, L.I.U. Feng, Z.H.U. Weichang, Q. Zhang, C.H.U. Xiangfeng, NdFeO₃ as anode material for S/O₂ solid oxide fuel cells. *J. Rare Earths* **30**(11), 1138–1141 (2012)
158. F. Wang, D. Chen, Z. Shao, Sm_{0.5}Sr_{0.5}Co_{0.3-δ}-infiltrated cathodes for solid oxide fuel cells with improved oxygen reduction activity and stability. *J. Power. Sources* **216**, 208–215 (2012)
159. R. Dittmer, E. Aulbach, W. Jo, K.G. Webber, J. Rödel, Large blocking force in Bi_{1/2}Na_{1/2}TiO₃-based lead-free piezoceramics. *Scripta Mater.* **67**(1), 100–103 (2012)
160. X.X. Wang, S.W. Or, K.H. Lam, H.L.W. Chan, P.K. Choy, P.C.K. Liu, Cymbal actuator fabricated using (Na_{0.46}K_{0.46}Li_{0.08})NbO₃ lead-free piezoceramic. *J. Electroceram.* **16**, 385–388 (2006)
161. S.K. Abbas, M.A. Aslam, M. Amir, S. Atiq, Z. Ahmed, S.A. Siddiqi, S. Naseem, Electrical impedance functionality and spin orientation transformation of nanostructured Sr-substituted BaMnO₃ hexagonal perovskites. *J. Alloy. Compd.* **712**, 720–731 (2017)
162. L.X. Zhang, W. Chen, X. Ren, Large recoverable electrostrain in Mn-doped (Ba, Sr) TiO₃ ceramics. *Appl. Phys. Lett.* **85**(23), 5658–5660 (2004)
163. S. Wada, K. Yako, H. Kakemoto, T. Tsurumi, T. Kiguchi, Enhanced piezoelectric properties of barium titanate single crystals with different engineered-domain sizes. *J. Appl. Phys.* **98**(1) (2005)
164. Z.Y. Shen, J.F. Li, Enhancement of piezoelectric constant d₃₃ in BaTiO₃ ceramics due to nano-domain structure. *J. Ceram. Soc. Jpn.* **118**(1382), 940–943 (2010)
165. D. Hu, K. Mori, X. Kong, K. Shinagawa, S. Wada, Q. Feng, Fabrication of [1 0 0]-oriented bismuth sodium titanate ceramics with small grain size and high density for piezoelectric materials. *J. Eur. Ceram. Soc.* **34**(5), 1169–1180 (2014)
166. T. Karaki, K. Yan, T. Miyamoto, M. Adachi, Lead-free piezoelectric ceramics with large dielectric and piezoelectric constants manufactured from BaTiO₃ nano-powder. *Jpn. J. Appl. Phys.* **46**(2L), L97 (2007)
167. M. Budimir, D. Damjanovic, N. Setter, Enhancement of the piezoelectric response of tetragonal perovskite single crystals by uniaxial stress applied along the polar axis: a free-energy approach. *Phys. Rev. B* **72**(6), 064107 (2005)
168. A. Kumar, A. Sharma, R. Kumar, R. Vaish, Finite element study on acoustic energy harvesting using lead-free piezoelectric ceramics. *J. Electron. Mater.* **47**, 1447–1458 (2018)
169. N.V. Volkov, Spintronics: manganite-based magnetic tunnel structures. *Phys. Usp.* **55**(3), 250 (2012)
170. X. Li, J. Yang, First-principles design of spintronics materials. *Natl. Sci. Rev.* **3**(3), 365–381 (2016)
171. H. Zabel, S.D. Bader, (eds.), Magnetic heterostructures: advances and perspectives in spinstructures and spintransport. (2007)
172. J.Z. Sun, L. Krusin-Elbaum, P.R. Duncombe, A. Gupta, R.B. Laibowitz, Temperature dependent, non-ohmic magnetoresistance in doped perovskite manganese trilayer junctions. *Appl. Phys. Lett.* **70**(13), 1769–1771 (1997)
173. M. Viret, M. Drouet, J. Nassar, J.P. Contour, C. Fermon, A. Fert, Low-field colossal magnetoresistance in manganite tunnel spin valves. *Europhys. Lett.* **39**(5), 545 (1997)

174. M. Bowen, M. Bibes, A. Barthélemy, J.P. Contour, A. Anane, Y. Lemaitre, A. Fert, Nearly total spin polarization in $\text{La}_{2/3}\text{Sr}_{1/3}\text{MnO}_3$ from tunneling experiments. *Appl. Phys. Lett.* **82**(2), 233–235 (2003)
175. U. Lüders, M. Bibes, K. Bouzehouane, E. Jacquet, J.P. Contour, S. Fusil, J.-f. bobo, j. fontcuberta, a. barthélemy and a. fert. *Appl. Phys. Lett.* **88**, 082505 (2006)
176. P. Fischer, M. Polomska, I. Sosnowska, M. Szymanski, Temperature dependence of the crystal and magnetic structures of BiFeO_3 . *J. Phys. C Solid State Phys.* **13**(10), 1931 (1980)
177. I. Fina, X. Marti, D. Yi, J. Liu, J.H. Chu, C. Rayan-Serrao, R. Ramesh, Anisotropic magnetoresistance in an antiferromagnetic semiconductor. *Nat. Commun.* **5**(1), 4671 (2014)
178. V. Baltz, A. Manchon, M. Tsoi, T. Moriyama, T. Ono, Y. Tserkovnyak, Antiferromagnetic spintronics. *Rev. Mod. Phys.* **90**(1), 015005 (2018)
179. J. Ryu, S. Lee, K.J. Lee, B.G. Park, Current-induced spin-orbit torques for spintronic applications. *Adv. Mater.* **32**(35), 1907148 (2020)
180. S. Ning, H. Liu, J. Wu, F. Luo, Challenges and opportunities for spintronics based on spin orbit torque. *Fundamental Res.* **2**(4), 535–538 (2022)
181. N.O. Urs, B. Mozooni, P. Mazalski, M. Kustov, P. Hayes, S. Deldar, J. McCord, Advanced magneto-optical microscopy: imaging from picoseconds to centimeters-imaging spin waves and temperature distributions. *AIP Adv.* **6**(5) (2016)
182. D. Xiong, Y. Jiang, K. Shi, A. Du, Y. Yao, Z. Guo, W. Zhao, Antiferromagnetic spintronics: an overview and outlook. *Fundamental Res.* **2**(4), 522–534 (2022)
183. N. Marati, R.G. Gupta, B. Vaithilingam, Multilayer ceramic capacitors crisis management in automotive industry. In 2020 IEEE International Conference on Power Electronics, Smart Grid and Renewable Energy (PESGRE2020), (IEEE, 2020) pp. 1–6
184. J. Zhang, Z. Pan, F.F. Guo, W.C. Liu, H. Ning, Y.B. Chen, Y.F. Chen, Semiconductor/relaxor 0–3 type composites without thermal depolarization in $\text{Bi}_0.5\text{Na}_0.5\text{TiO}_3$ -based lead-free piezoceramics. *Nat. Commun.* **6**(1), 6615 (2015)
185. J. Zhang, Z. Pan, P.X. Nie, Y.S. Cui, B. Yang, J. Chen, S.T. Zhang, $\text{Bi}_0.5\text{Na}_0.5\text{TiO}_3$: ZnO lead-free piezoelectric composites with deferred thermal depolarization. *Appl. Phys. Lett.* **106**(23) (2015)
186. P. Peng, H. Nie, Z. Liu, W. Ren, F. Cao, G. Wang, X. Dong, Enhanced ferroelectric properties and thermal stability of Mn-doped 0.96 ($\text{Bi}_0.5\text{Na}_0.5\text{TiO}_3$ -0.04 BiAlO_3) ceramics. *J. Am. Ceram. Soc.* **100**(3), 1030–1036 (2017)
187. X. Liu, X. Tan, Giant strains in non-textured $(\text{Bi}_{1/2}\text{Na}_{1/2})\text{TiO}_3$ -based lead-free ceramics. *Adv. Mater.* **28**(3), 574–578 (2016)

Springer Nature or its licensor (e.g. a society or other partner) holds exclusive rights to this article under a publishing agreement with the author(s) or other rightsholder(s); author self-archiving of the accepted manuscript version of this article is solely governed by the terms of such publishing agreement and applicable law.